Energy Systems
https://doi.org/10.1007/s12667-023-00614-y

ORIGINAL PAPER

Optimal price-based scheduling of a pumped-storage hydropower plant considering environmental constraints

Asja Alic[1] · **Linn Emelie Schäffer**[2,4] · **Marco Toffolon**[1] · **Vincenzo Trovato**[1,3]

Received: 2 December 2022 / Accepted: 6 August 2023

Abstract

The paper proposes a novel medium-term scheduling model for a hydropower system composed by a pumped storage hydropower plant connected to a traditional hydropower plant subject to three types of environmental constraints; these deal with the maximum water abstraction from the reservoir thought the turbines and through the pump for energy production, the minimum environmental water flow and the ramping capabilities of water volumes inside the system's reservoirs. The scheduling problem is formulated for a planning horizon of 1 year with weekly decision stages. The methodology to determine the optimal operation of the plant is based on a stochastic dynamic programming algorithm which allows for an accurate representation of the uncertainties associated to the water inflows and energy prices. Moreover, it facilitates the handling of the non-convex characteristic of the state-dependent constraint on maximum water abstraction from the reservoir. The model is applied to the case of a real hydropower system based on a cascaded watercourse with two conventional hydropower plants in south of Norway to assess the economic benefits of having a pumping unit and the technical impact of the above-mentioned environmental constraints. Furthermore, this work proposes a methodology to analyze the optimal operation of the hydropower system, computed for different temporal resolutions, in order to investigate the techno-economic impact of the constraints involving dependencies on the states of the system, the different environmental constraints and other seasonal effects on the accuracy and the applicability of medium-term scheduling models. Further case studies assess the computational burden and the precision of the results when adopting a finer discretization of the state variables of the dynamic-programming-based methodology.

Keywords Pumped storage hydropower plant · Optimal hydropower scheduling · Environmental constraints · Electricity markets · Stochastic dynamic programming

Abbreviations

BC	Base Case
FS	Forward Simulation

Extended author information available on the last page of the article

Published online: 28 September 2023

GHG	Green House Gases
HPP	Hydropower Plant
MEF	Minimum Environmental Flow
PSHP	Pumped Storage Hydropower Plant
RES	Renewable Energy Sources
SCWA	State-dependent Constraint on Maximum Water Abstraction
SDP	Stochastic Dynamic Programming
WVs	Water Values

Sets

$\mathcal{D}_h$	Set of discharge segments from turbine per hydropower plant h
$\mathcal{E}_{\overline{h}}$	Set of pumped-water segments from pump in the upstream hydropower plant $\overline{h}$
$\mathcal{H}$	Set of hydropower plants
$\mathcal{I}$	Set of sub-intervals within each daily stage z
$\mathcal{J}$	Set of iterations in SDP algorithm
$\mathcal{K}$	Set of sub-intervals within each weekly stage t
L	Set of stochastic states per stage t
$\mathcal{N}$	Set of discrete reservoir segments per reservoir
$\mathcal{S}^p$	Set of endogenous states–reservoirs' volumes
$\mathcal{S}^u$	Set of all stochastic states–weekly water inflows and average weekly energy prices
$S^u_{h,t}$	Subset of stochastic states for reservoir h in stage t
$\mathcal{T}$	Set of weekly stages
$\mathcal{T}_{env}$	Subset of weeks during which the state-dependent constraint on maximum water abstraction is active
$\mathcal{T}_{MEF}$	Subset of weeks during which the minimum environmental flow is required
$\mathcal{Z}$	Set of daily stages

Indexes

d	Index for discharge segment for turbines
e	Index for pumped-water segment for pumps
h	Index for hydropower plant
i	Index for the sub-interval within stage z
l	Index for stochastic state in reservoir h within stage t
k	Index for the sub-interval within stage t
m	Index for volume segment in upper reservoir
n	Index for volume segment in lower reservoir
r	Index for water volume intervals for the evaluation of ramping constraints
t	Index for weekly stage
z	Index for daily stage

Decision variables

$b_{h,k}$	Variable for minimum environmental flow from reservoir h, in sub-interval k [m^3/s]

$f_{h,k}$	Spillage from reservoir h, in sub-interval k [m^3/s]
$p_{h,k}$	Generated power from reservoir h, in sub-interval k [MW]
$pp_{\overline{h},k}$	Power absorbed by the pump in the upstream reservoir $\overline{h}$, in sub-interval k [MW]
$q_{h,k,d}$	Water discharge from turbine in sub-interval k, segment d from reservoir h [m^3/s]
$qp_{\overline{h},k,e}$	Water pumped from pump in sub-interval k, segment e from the upstream reservoir $\overline{h}$ [m^3/s]
$res^{+}_{h,k}$	Slack variable for positive volume variations for reservoir h, in sub-interval k [Mm^3]
$res^{-}_{h,k}$	Slack variable for negative volume variations for reservoir h, in sub-interval k [Mm^3]
$mef_{h,k}$	Slack variable for minimum environmental flow for reservoir h, in sub-interval k [m^3/s]
$v_{h,k}$	Water volume in reservoir h, at the end of sub-interval k [Mm^3]
α_{t+1}	Expected future revenue at stage t [€]
$\gamma_{n,m}$	Weighting variable for reservoir segments n, m

Parameters

C^c	Penalty cost for slack variables [€/m^3/s]–[€/Mm^3]
C^s	Penalty cost for spillage [€/m^3/s]
E	Number of segments of the approximating piecewise liner function of the pump unit
F^H	Conversion factor, number of hours in each sub-interval k [h]
F^C	Conversion factor, flow to volume [$Mm^3/m^3/s$]
F^z	Conversion factor, number of hours in each sub-interval z [h]
$FV_{n,m}$	Expected future revenue points for reservoir segments n and m [€]
I	Number of sub-intervals in each daily stage z
J	Maximum number of iterations in SDP algorithm
K	Number of sub-intervals in each weekly stage t
L	Number of states in each weekly stage t
N	Number of discretization points per reservoir
N_r	Number of water volume intervals for the evaluation of ramping constraints
$pp^{max}_{\overline{h},e}$	Maximum power absorbed by pump in the upstream reservoir $\overline{h}$ and pumped-water segment e [MW]
Pd_h	Parameter for pump direction
Q^{min}_h	Minimum environmental flow from hydropower plant h [m^3/s]
$Q^{max}_{h,d}$	Maximum discharge from turbine per reservoir h and discharge segment d [m^3/s]
$QP^{max}_{\overline{h},e}$	Maximum pumped water from pump in the upstream reservoir $\overline{h}$ and pumped-water segment e [m^3/s]
s^p	Endogenous state
$s^u_{h,t,l}$	Stochastic state l at stage t per hydropower plant h
T	Number of stages in yearly-planning horizon

$\overline{v}_{h,0}$	Initial water volume in reservoir h for week $t = 1$ [Mm^3]
$V_{\underline{h}}^{lim}$	Environmental threshold for the downstream reservoir $\underline{h}$ [Mm^3]
V_h^{max}	Maximum storage volume in reservoir h [Mm^3]
V_h^{min}	Minimum storage volume in reservoir h [Mm^3]
$\underline{V}_{\underline{h}}$	Threshold volume in the downstream reservoir $\underline{h}$ for pumping [Mm^3]
$Y_{h,t}$	Total weekly water inflow to reservoir h at stage t [Mm^3]
$Y_{h,z}$	Total daily water inflow to reservoir h at stage z [Mm^3]
Z	Number of stages in weekly-planning horizon
$\delta_{h,k}$	Net water head for hydropower h, in sub-interval k [m]
Δ_j^{wv}	Change in Water Value matrix in iteration j €/Mm^3]
ε	Convergence tolerance for WVs [€/Mm^3]
ϵ_h	Deviation index for reservoir h [Mm^3]
$\eta_{h,d}$	Performance slope for turbines per hydropower plant h and discharge segment d [MW/m^3/s]
$\eta p_{\overline{h},e}$	Performance slope for pump in the upstream hydropower plant $\overline{h}$ and segment e [m^3/s/MW]
$\theta_{t,k}$	Scaling factor for price variability in sub-interval k for stage t
$\theta_{z,i}$	Scaling factor for price variability in sub-interval i for stage z
λ_t	Weekly average energy price at stage t [€/MWh]
λ_z	Daily average energy price at stage z [€/MWh]
$\sigma_{h,N}^s$	Water volume for reservoir h per segment s and N discretization points [Mm^3]
υ_l^+	Maximum water level increase for ramping constraints [m]
υ_l^-	Maximum water level decrease for ramping constraints [m]
υ_v^+	Maximum water volume increase for ramping constraints [Mm^3]
υ_v^-	maximum water volume decrease for ramping constraints [Mm^3]
$\varphi_{h,k}$	Distribution factor of inflow to each sub-interval k in reservoir h
$\Psi_{j,t}^h(\dots)$	Water value matrix for reservoir h, stage t, iteration j
$\overline{\omega}_{h,N}^s$	Upper extreme for the water segment s in hydropower plant h, for N discretization points [Mm^3]
$\underline{\omega}_{h,N}^s$	Lower extreme for the water segment s in hydropower plant h, for N discretization points [Mm^3]

1 Introduction

The penetration of Renewable Energy Sources (RES), such as wind and solar energy, in the several power systems worldwide have reached a remarkable share contributing to the reduction of Green House Gas emissions (GHG) stemming from conventional thermal power plants [1, 2]. However, the uncertainty and intermittency of their outputs and the lack of support to the system inertial response [3] may affect the system frequency stability since the existing protection schemes might fail

to operate because of their pre-set condition [4, 5]. To mitigate these shortcomings and provide safe operation and control of power systems, additional and appropriate control schemes and ancillary services are needed. Furthermore, power system operators may require energy storage technologies and adequate management strategies to flexibly change their generation/demand output and provide ancillary services to the power systems. Pumped Storage Hydropower Plants (PSHPs) are nowadays one of the most mature and most spread technologies for energy storage [6]. The basic principle relies on the movement of water between two interconnected reservoirs, which are located at different altitudes. A volume of water may be diverted from the upper reservoir through a penstock to spin a hydraulic turbine coupled to a synchronous generator in order to produce electrical energy (discharge phase). Afterwards, the system may absorb electrical energy to spin a hydraulic pump to move the volume of water from the lower reservoir back to the upper one (recharge phase) [7]. The opportunity to pump water towards the upper reservoir allows to store potential energy associated to a volume of water at a certain altitude and use this energy, later when needed, to produce electricity. Their round-trip efficiency, which indicates the percentage of the stored energy that can be retrieved later [8] may reach 80%—depending on site-specific conditions [6]. Moreover, the typically large water storage capacities of PSHPs make these systems suitable for energy-shifting over short-, medium- and long-term horizons [6]. On the one hand, PSHPs can produce energy if the power system position is *short* (the total demand exceeds the generation e.g. due to a lack of wind/solar generation). On the other hand, PSHPs absorb energy, while in pumping operation, to help the power system cope with *long* positions (the total generation is higher than the demand e.g., due to extra-availability of RES).

Such flexible operation of PSHPs may provide economic benefits. In fact, PSHPs may engage in energy arbitrage, operating in pump-mode in moments of low energy prices and operating in turbine-mode when the energy prices are higher. While contributing to secure integration of uncertain and intermittent RES in power system, PSHPs might therefore give also significant potential economic advantages.

Even though traditional hydropower plants (HPPs)—with no pumping capabilities—and PSHPs might play a key role in the energy transition, they have a non-negligible impact on the surrounding ecosystems [9, 10] which must be considered when operating the existing hydropower systems or before constructing new ones. HPPs and PSHPs may modify both the morphology and the hydrodynamics inside the reservoirs as well as the flow regimes and the water quality of downstream watercourses [11]. The construction of dams and artificial reservoirs reduces the connectivity of aquatic systems, altering the flow regimes and causing hydropeaking phenomena. Consequently, non-natural hydropower waterflows may endanger floodplains, threaten fish, bird species and facilitate erosion processes [9]. These effects might be even more relevant in PSHPs where a pumping system is present. As a matter of fact, a more frequent movement of water between two interconnected reservoirs might increase both the frequency and the magnitude in the water level variations inside each of the reservoirs [11]. Furthermore, the vertical mixing of water volumes can alter the thermal structure, deep water mixing processes and water circulation characteristics [12]. Consequent changes in stratification can modify the water quality, the oxygenation and the nutrient concentration inside the water bodies

which in turn might affect aquatic species and the wildlife [12]. Especially during winter periods, also the stability of the ice cover of the reservoirs might be affected by these variable and frequent water fluctuations [13].

To mitigate these shortcomings and preserve the sustainment of the local flora and fauna, several site-specific environmental restrictions might be imposed by the national regulators or by the hydropower producers themselves as a voluntary act [14]. To find an efficient and sustainable trade-off between power production and the requirements on environmental flows, these environmental regulations must be precisely modelled and implemented as constraints in scheduling models. Among others, the minimum environmental flow (MEF) and the ramping constraints are the most commonly applied in HPPs and they are already adopted by many European countries. Note that MEF indicates the minimum amount of water that must be released from the reservoirs to preserve the quality of watercourses downstream the hydropower plants. The ramping constraints limit the variations of the flow downstream the outlet of the HPPs or the water level fluctuations inside the reservoir below a certain threshold. In addition, there are other types of environmental constraints known as "state-dependent" constraints, which are already widely used in Norwegian hydropower systems. Differently from the previous constraints, the state-dependent constraints are strictly dependent on the values of one or more state variables of the system, e.g., incoming water inflows and reservoirs' volumes [15]. Moreover, they can be enforced or not or even simply modified in accordance with specific logical conditions and/or within determined periods of the year [16]. It is easy to be convinced that the application of any environmental constraint eventually decreases the possible operation of the PSHP, restricting the set of feasible solutions for the optimal sequence of operations of the power plant. This, in turn, would reduce the associated revenue for the system.

1.1 Context and related works

In light of the techno-economic and environmental considerations above, the assessment of the optimal operation of hydropower systems becomes crucial [17]. In general, the assessment of the optimal operation of a HPP over a certain horizon is subject to external uncertainties such as water inflows, snow storage and wholesale energy prices which in turn depend on other issues such as the available energy mix [18]. The modelling of these uncertainties into an optimal scheduling model depends on the length of the considered horizon. It is common to refer to long-, medium- and short-term optimal scheduling models for HPPs [19]. Long-term scheduling models are typically stochastic models used to make forecast on future energy prices, water inflows and energy production and they have typical scheduling horizon of 1–10 years. Medium-term models instead are used to evaluate the optimal management of the water volumes inside the reservoirs under inflow and price uncertainty for a planning horizon of few months up to a year [20]. Short-term scheduling models consider shorter periods of days or weeks during which the modelling and impact of certain uncertainties can be

neglected. In fact, differently from the long- and medium- term models, short-term scheduling problems are deterministic models [17]. The optimal scheduling model developed in the proposed paper belongs to the category of medium-term problems.

Furthermore, it is worth pointing out that the assessment of the optimal operation of a HPP, e.g., in order to maximize the revenues, may not be trivial when state-dependent constraints are enforced. This is because of the specific formulation of these constraints which would eventually make the overall optimization problem non-convex and thus hard to be solved. One practical example is the state-dependent constraint on maximum water discharge, which prohibits the discharge of water through the turbines for energy production when the water levels of the reservoirs are below a certain threshold. This constraint aims to retain water during summer periods when inflows are abundant in order to satisfy both the ecological and recreational needs for high water levels during spring-summer seasons.

Previous works have demonstrated that the Stochastic Dual Dynamic Programming (SDDP) is the most effective methodology in the field of the medium-term (and long-term) scheduling models for a hydropower system [21]. In addition, another methodology—the Stochastic Dynamic Programming (SDP)—stands out in literature as an effective tool when models are characterized by pronounced non-convexities. The SDP is an efficient tool for solving sequential optimization problems—such as hydropower scheduling problems involving multi-stage decision processes—by decomposing the main optimal control problem into smaller optimization problems, according to Bellman's principle of optimality [22]. Furthermore, the SDP algorithm facilitates the implementation of constraints involving time and state-dependent logical conditions—which in turn might result in non-convex mathematical formulations—and enables the representation of uncertainties such as water inflows and energy prices [20]. Finally, the SDP algorithms are suitable for small systems involving a limited number of state variables due to the intrinsic large computational capability required.

Two interesting and similar applications of the SDP are in [23] and [24] where the operational profitability of a hydropower system selling both energy and reserve capacity in a competitive market setting is presented. A mathematical model based on SDP is used to compute the Water Values (WVs) for the hydropower system. An effective extension of the SDP method, especially for large watersheds with multidimensional inflows, is the *sampling*-SDP. As opposed to SDP, the WV function with the sampling-SDP depends on the index of an inflow scenarios. The optimization is therefore performed by using the inflow sequences directly rather than statistical models of the inflow scenarios. An application of this methodology to a real hydropower system in Canada is presented in [25]. Finally, a deterministic formulation of a discrete dynamic programming methodology to consider the variability and uncertainty of water inflows and market energy prices is adopted in [26].

The medium-term optimal scheduling model proposed in this paper relies on the use of the SDP methodology. The choice is driven by the presence of non-convex and state-dependent environmental constraints. Moreover, it is worth noting that the analysis of the integration of the environmental constraints developed in this paper

within alternative methodologies (e.g., stochastic dual dynamic integer programming or sampling-SDP) is beyond the scope of the paper.

Concerning the integration of environmental restrictions, previous studies have investigated the implementation of site-specific environmental constraints in optimal scheduling models for traditional HPPs and how they can affect the hydropower system operation. The methodologies developed in [26–28] have explored the economic impacts of MEF and of ramping constraints both on the WVs and on the annual operation of conventional HPPs. Results in [27] have evidenced how the implementation of such constraints can significantly affect the WVs which tend to increase with a larger MEF and decrease with more severe ramping constraints. In particular, the influence of MEF is stronger during the wettest seasons while the impacts of ramping constraints are more pronounced during the driest periods. Note that the MEF—which usually has the highest values during spring and summer—can be seen as a reduction in the reservoir level which is reflected as an increase in the WVs. Additionally, [26] has demonstrated how the annual losses in energy production and revenues increase quadratically as function of ramping constraints and increase almost linearly as function of MEF. Instead, the authors of [28] have found that ramping constraints can negatively affect the overall revenue by redistributing the power generation from periods of high energy prices to periods of lower energy prices but may give an increase in the total energy production.

On the other hand, [20] and [29] have investigated how the presence of state-dependent constraints on maximum water discharge can affect the water management inside the reservoir and the WVs themselves, especially during the restriction period. Results in [20] have shown that the state-dependent constraint on maximum discharge significantly impacts the WVs and therefore the operation of the system. Specifically, simulation results have shown that systems subject to this constraint exhibit an overall decrease in both the total energy production and in the revenues. Instead, the outcomes of [29] have evidenced how a tighten linear approximation can lead to a more accurate model representation and improvement in the system operation.

1.2 Contributions

This paper provides clear contribution to the existing literature. The initial methodology developed in [20] is effectively extended to produce a novel medium-term scheduling model for a hydropower system composed by a PSHP and a traditional HPP. Furthermore, the system is subject to state-dependent constraints on maximum water release throught both the turbines and the pump unit and two additional environmental constraints: the constraints on MEF and on the ramping characteristics. It must be pointed out that the original model considered only the state-dependent constraint on maximum discharge for a traditonal HPP—thus limiting the discharge of water through the turbines for power production. The addition of a pumping unit required therefore the re-formulation of the state-dependent constraint on maximum discharge in order to consider also the

maximum water allowed to be pumped by the pump during the restriction period. To highlight this fundamental modelling advancement, the present work refers to this constraint as "state-dependent constraint on maximum water abstraction" (SCWA), thus considering both the water discharged through the turbines and the water pumped by the pump unit.

The novel medium-term stochastic scheduling model allows therefore the assessment of the optimal techno-economic operation of a hydropower system that aims to maximize the potential economic revenue while respecting the three above-mentioned environmental restrictions. The impact of these limitations is evaluated also considering the effect in PSHP operation on the sorrounding ecosystem. The SDP algorithm is used to evaluate the solution strategy for a hydropower system based on a cascaded watercourse composed by two interconnected reservoirs with relative power stations, enabling the representation of the uncertainties of water inflows and energy prices and facilitating the resolution of non-convexities present in the problem formulation due to state-dependent constraint on maximum water abstraction.

The main contributions of this paper can be summarized as follows:

1. The first contribution deals with the modelling of the optimal scheduling algorithms. The original medium-term scheduling model—developed for a cascade system of two traditional HPPs—has been extended to include a pumping unit. Moreover, the model considers the simultaneous presence of three environmental constraints: (i) a constraint on MEF, (ii) a set of constraints on the variations on the water level fluctuations inside the reservoir and (iii) a SCWA from the reservoir. To the best of the authors' knowledge, the implementation of the above-mentioned constraints to a hydropower system with a PSHP has not been formulated and tested in previous works. Similarly, previous works did not implement the three above-mentioned constraints, simultaneously.
2. The second contribution is the analysis on the actual ability to effectively ensure state-dependent constraints over different optimization horizons (e.g., weekly and daily horizons). In fact, due to their strict dependence on the knowledge and value of the state variables, the effectiveness of specific state-dependent constraints reduces when considering a weekly-resolution, leading to an under- or over-estimation of the weekly energy production and revenues. Therefore, the proposed work investigates how specific state-dependent constraints might be enforced more precisely because of a more frequent knowledge of the state variables and the consequent changes in the system operation. In other words, this paper proposes a novel methodology which, without introducing any computational burden, may effectively combine the typical framework of a mid-term scheduling model with the benefits of a more rapid optimal setting of the state variables.
3. The proposed model is applied to a real hydropower system located in south of Norway to assess the potential increase in annual revenues by adding a pumping unit in a conventional hydropower plant. Moreover, the study evaluates the changes in operation, energy production and expected revenues of the hydropower system (both in traditional and pumping mode) when considering the presence of ramping constraints. Finally, the case studies investigate the effectiveness on the interpolation procedure for the calculation of the water volumes varying the

fundamental features of the SDP algorithm e.g., the granularity of the discretization of the state variables.

This paper is organized as follows: Sect. 2 provides with an overview of the structure of the model, describing the considered hydropower system (Sect. 2.1) and explaining the use of the SDP algorithm for the calculation of WVs (Sect. 2.2) and the use of a Forward Simulation (FS) algorithm to assess the optimal operation of the hydropower system (Sect. 2.3). Section 3 deals with a description on the new modelling features (3.1 and 3.2) and describes in detail the mathematical formulation of the optimization problem (3.3). Section 4 proposes a new methodology based on the features of the medium-term scheduling to simulate the operation of a hydropower system with daily stages. The case studies used to validate the model and the obtained results are reported in Sect. 5. Conclusive remarks are addressed in Sect. 6.

2 Methodology

The proposed medium-term scheduling model is used to compute the optimal operation of a PSHP connected to a traditional HPP. The planning horizon is 1 year with weekly decision stages. The objective is to maximize the operational revenues whilst considering the presence of stochastic variables (i.e., water inflows and energy prices) and fulfilling technical and environmental constraints.

For this purpose, the proposed model requires the consecutive resolution of two algorithms: the SDP algorithm and the FS algorithm. The overall description of the resolution process is illustrated in Fig. 1.

The SDP algorithm solves the scheduling problem for each stage while considering all states of the model, i.e., the water inflows, wholesale energy prices and water volumes inside the reservoirs. For each combination of stages and states, the SDP algorithm calculates the relative WVs which inform on the optimal management of the water sources inside the reservoirs. The algorithm is solved backwards, starting

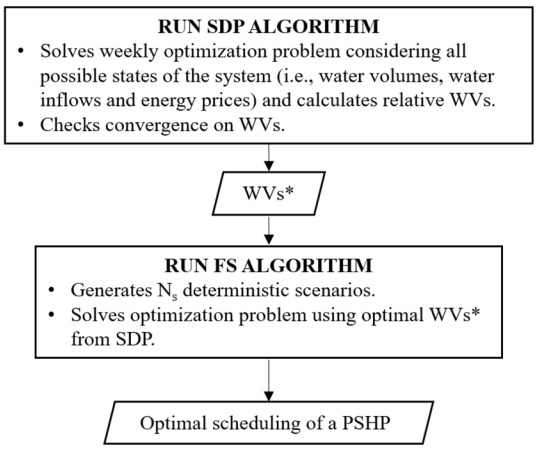

Fig. 1 Model structure and resolution process of the SDP and FS algorithms

from the end of the planning horizon, until convergence on the WVs is reached. Afterwards, the FS algorithm generates and simulates a certain number N_s of deterministic scenarios in which the water inflows and energy prices are known before the weekly optimization problem is solved. Based on the optimal values of WVs (denoted with a star WVs* and being outputs of the SDP algorithm), the FS algorithm optimizes the system's operation and computes the expected revenues. Specific details on each of the algorithms are reported in the following.

2.1 Hydropower system description

In general, a watercourse is referred to a set $\mathcal{H}$ of interconnected HPP where each HPP, indexed by $h \in \mathcal{H}$, is composed by a reservoir, a penstock, and a powerhouse. Part of the water may be released from the reservoir though the penstock towards the turbine in the powerhouse, spinning it to activate a generator to produce electricity. Furthermore, a powerhouse may be equipped with a pump: by absorbing electrical energy from the power grid, the pumping machine allows for the water to be sent back to the reservoir of the plant. This setup is referred to a PSHP.

The presented medium-term scheduling model considers a hydropower system based on a watercourse composed by two cascaded interconnected plants such that $\mathcal{H} = \left\{\overline{h}, \underline{h}\right\}$. The upstream one is indicated with $h = \overline{h}$ and it is a PSHP; it discharges the spilled water and the water used for energy production directly into the downstream reservoir denoted with $h = \underline{h}$. Furthermore, given the presence of a pumping machine in the upper powerhouse $\overline{h}$, the movement of water is also allowed from the reservoir $\underline{h}$ to the upper one $\overline{h}$. The downstream plant $\underline{h}$ is a traditional HPP which discharges the spilled water and the water flowing through the turbines to produce electricity.

Moreover, as explained in Sect. 1.2, the proposed model considers that only the downstream reservoir $\underline{h}$ is subject to the SCWA.

2.2 Stochastic dynamic programming algorithm

The objective of the SDP algorithm is the evaluation of the optimal WVs at each stage $t = \{1, \ldots, T\}$ of the optimization horizon. In this work, the optimization horizon is chosen to be 1 year with weekly decision stages t, thus leading to $T = 52$. Furthermore, each of the stages t is divided into $K = 56$ sub-intervals of three hours length, indexed by $k = \{1, \ldots, K\}$.

The WVs are expressed in €/Mm^3 since they have an economic meaning. In fact, they represent the marginal value of storing water in a reservoir of a hydropower system. In accordance with the definition proposed in [30], the WVs represent the opportunity cost associated with the water stored in the reservoirs. The producer may decide to use the available water in the reservoir to direct energy towards the main power grid and collect revenues for it or store the water and use it at a later stage with a potential increase in profit. Note that, the WVs tend to decrease with increasing water volumes because the risk of spillage is higher, on the other hand

they tend to increase for low storage volumes because of a higher risk of emptying the reservoirs. Therefore, the knowledge of WVs at each of the weekly stages t allows for an optimal management of the water volumes inside the reservoirs.

The SDP algorithm requires the definition of the state variables, which contain the main information of the system between one stage $t-1$ and the next one t. In this case, the set of state variables is made of two subsets: the first subset refers to the *endogenous* variables of the system ($\mathcal{S}^p$) while the second one considers the *exogenous* and stochastic variables ($\mathcal{S}^u$) [20]. The endogenous state variables are the water volumes of the upper ($\overline{h}$) and of the lower ($\underline{h}$) reservoirs. Furthermore, as typically done for dynamic programming problems, these states are discretised. In this work, both the upper and the lower water volumes are equally divided into N equidistant points leading to a total of N^2 possible water volume combinations. The exogenous stochastic state variables are considered for each of the reservoirs h and at each stage t. Hence, a subset ($S^u_{h,t} \in \mathcal{S}^u$) containing five possible states, indexed by $l = \{1, \dots, L\}$ with $L = 5$, is considered. Each of the L states comprises a pair of values: the total weekly inflow for each of the reservoirs $(Y_l)_{h,t}$ [Mm^3] and the corresponding average weekly wholesale energy prices $(\lambda_l)_t$ [€/MWh]—as expressed in (1). It is worth noting that the weekly energy prices are the same for both the reservoirs.

$$S^u_{h,t} = \left\{ Y_1, \dots Y_l, \dots Y_L; \lambda_1, \dots, \lambda_l, \dots \lambda_L \right\}_{h,t} \tag{1}$$

The stochastic variables are modelled as discrete nodes using a discrete Markov chain [20]. This model receives as input several annual historical data of weekly inflows together with weekly average energy prices corresponding to the same weeks. A serial correlation between the inflows of two adjacent weeks t and $t+1$ is evaluated, while a cross-correlation is calculated between the weekly inflows and the corresponding prices. For each week t, 10000 points—corresponding to a combination of water inflows and relative energy prices—are sorted from the autoregressive model and grouped into five discrete nodes, using a *K-means clustering* algorithm [31]. The transition probabilities from one state to another are determined by counting the shares of scenarios transitioning between different nodes, from one week to the next one [20].

The SDP algorithm solves the revenue-maximization problem described in Sect. 3.3 and calculates the WVs for each of the reservoirs ($h \in \mathcal{H}$), at each of the weekly stages ($t \in \mathcal{T}$) and for all the reservoir volume combinations ($s^p \in \mathcal{S}^p$) and stochastic states ($s^u_{h,t,l} \in S^u_{h,t} \subset \mathcal{S}^u$) of the model.

The evaluation of the WVs requires an iterative strategy since the WVs are unknown at the beginning of the procedure. In other words, the SDP algorithm is solved J times until a certain degree of convergence concerning the WVs is reached. At the first iteration ($j = 1$), the WVs for the last stage T are initialized to zero ($WV_{j=1,t=T} = 0$). Afterwards, within each iteration $j \in \mathcal{J}$, the SDP algorithm is solved backwards, i.e. starting from the final stage T up to the initial one, iterating over all reservoirs h, water volume states s^p and their stochastic states $s^u_{h,t,l}$ as illustrated in a simplified form in Fig. 2. Further explanations on the solution strategy can be found in [20].

The convergence of the SDP algorithm is checked by means of the stopping criterium (2) as done in [23], which evaluates whether Δ_j^{wv}, i.e. the absolute value

Stochastic Dynamic Programming (SDP) Algorithm

$j \leftarrow 0, \Delta_j^{wv} \leftarrow \infty, \Psi^h_{j,t=T}(\ldots) \leftarrow 0$

while $\Delta_j^{wv} > \varepsilon$ *or* $j < J$

  for $t = T : -1 : 1$

    for $h \in H$

      for $s^p \in S^p$

        for $s^u_{h,t,l} \in S^u_{h,t} \subset S^u$

- prepare input: s^p, $s^u_{h,t,l}$, $\Psi^h_{j,t+1}(\ldots)$
- run Scheduling Algorithm
- calculate WVs and store in matrix $\Psi^h_{j,t}(\ldots)$

        end for

      end for

    end for

  end for

$\Delta_j^{wv} \leftarrow |\Psi^h_{j,t=T}(s^p, s^u_{h,t,l}) - \Psi^h_{j,t=0}(s^p, s^u_{h,t,l})| \quad \forall s^p \in S^p, \forall s^u_{h,t,l} \in S^u_{h,t} \subset S^u, \forall h \in H$

  if $\Delta_j^{wv} > \varepsilon$ **then**

$\Psi^h_{j+1,t=T}(s^p, s^u_{h,t,l}) = \Psi^h_{j,t=0}(s^p, s^u_{h,t,l}) \quad \forall s^p \in S^p, \forall s^u_{h,t,l} \in S^u_{h,t} \subset S^u, \forall h \in H$

  end if

end while

Fig. 2 Pseudocode of the SDP Algorithm scheme

of the difference between the WVs at $t = T$ and $t = 0$ at the end of iteration j, is smaller than a given tolerance ε:

$$\Delta_j^{wv} = \left|\Psi^h_{j,t=T}\left(s^p, s^u_{h,t,l}\right) - \Psi^h_{j,t=0}\left(s^p, s^u_{h,t,l}\right)\right| \leq \varepsilon \quad \forall s^p \in \mathcal{S}^p, \forall s^u_{h,t,l} \in S^u_{h,t} \subset \mathcal{S}^u, \forall h \in \mathcal{H} \tag{2}$$

Where $\Psi^h_{j,t}(\ldots)$ indicates the matrix storing the values of WVs expressed in €/Mm^3 for reservoir h, stage t at iteration j. If convergence is reached, the iterative procedure stops. If not, (3) applies, where the WVs obtained from the first stage in iteration j ($WV_{j,t=0}$) are used as WVs for the last week T in the next iteration $j + 1$ (i.e. $WV_{j+1,t=T}$). This is to implement an infinite-planning horizon formulation i.e., assuming periodic yearly boundary conditions.

$$\Psi^h_{j+1,t=T}\left(s^p, s^u_{h,t,l}\right) = \Psi^h_{j,t=0}\left(s^p, s^u_{h,t,l}\right) \quad \forall s^p \in \mathcal{S}^p, \forall s^u_{h,t,l} \in S^u_{h,t} \subset \mathcal{S}^u, \forall h \in \mathcal{H} \tag{3}$$

2.3 Forward simulation algorithm

In accordance with Fig. 1, the FS algorithm computes the optimal operation of the combined plants of the considered hydropower system.

As explained in Fig. 3, for each generated scenario N_s, the FS solves the deterministic weekly optimization problem by running the Scheduling Algorithm in Sect. 3.3 for each reservoir h, starting from the first week of the year $t = 1$ till the last one $t = T$, and adopting the corresponding optimal WVs* obtained from the SDP algorithm. As a matter of fact, the states of the system, i.e., the water volumes in the reservoirs at the end of the previous stage $v^{t-1}_{h,k=K}$, the total weekly water inflows $Y_{h,t}$ and average weekly energy prices λ_t, are now known quantities at the beginning of each stage t and given as input to the weekly-decision problem.

Hence the FS algorithm evaluates the optimal amount of water that must be released from the reservoirs for energy production ($q^*_{h,k,d}$) and optimal amount of water pumped by the pump unit ($qp^*_{h,k,e}$) at each sub-interval k.

Forward Simulation (FS) Algorithm

for $n = 1 : N_s$
  for $t = 1 : T$
    for $h = 1 : H$
    - prepare input: $Y_{h,t}$, λ_t, $v^{t-1}_{h,k=K}$, $\Psi^h_{j,t+1}(...)$
    - run Scheduling Algorithm

    end for
  end for
end for

Fig. 3 Pseudocode of the FS Algorithm

3 Modelling and formulation of the scheduling problem

3.1 Pumping system

The proposed formulation of the PSHP adopts a modelling simplification of ignoring the grid-connection configuration and types of electrical machines (e.g., fixed-speed pumps vs. fully-fed or doubly-fed electrical machines). This allows to quantify a common overall upper bound for the flexibility and the additional value that can be provided by the PSHP whilst respecting fundamental environmental constraints. It is worth noting that the flexible operation of the pump unit enabled in this work better resembles the features of a fully-fed or doubly-fed electric machine rather than a fixed-speed pump. Within this context, the first additional feature introduced in this paper is the modelling of the pumping system to upgrade the upstream traditional HPP to a PSHP. While in pumping operation, the pump installed in the upstream power station $\overline{h}$ would move a volume of water from the corresponding downstream reservoir $\underline{h}$.

To do so, at each sub-interval k, the pump requires the absorption of electric power $pp_{\overline{h},k}$ which is a function of the pumped water $qp_{\overline{h},k}$, the net head $\delta_{\overline{h},k}$ and the pump efficiency $\eta p_{\overline{h},k}$. The dependency of $pp_{\overline{h},k}$ from the recalled parameters is non-linear e.g., due to the non-linear variation of the pump efficiency $\eta p_{\overline{h},k}$ with respect to the net head $\delta_{\overline{h},k}$ and on the pumped water $qp_{\overline{h},k}$. In accordance with the modelling assumptions of the turbines in [20], the proposed model neglects the net head variations with respect to the gross head available. This assumption if often implemented in medium-term scheduling models and lets the electric power $pp_{\overline{h},k}$ be expressed by means of a single curve as the blue dotted one in Fig. 4. This curve can be therefore approximated by a concave piece-wise linear function (red solid line in Fig. 4).

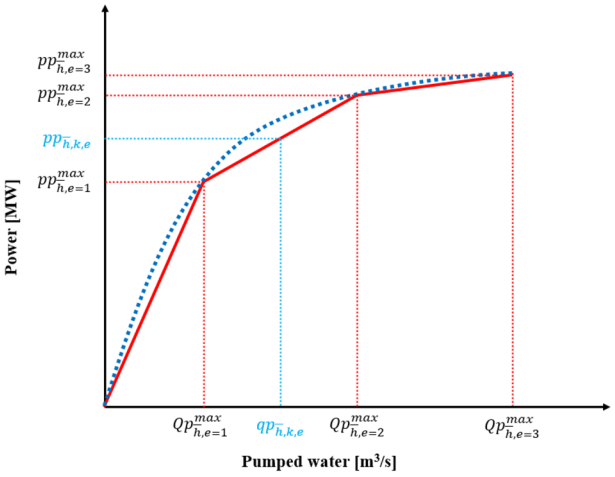

Fig. 4 Concave piecewise linear function modelling the relationship between the power consumption of the pump and the corresponding pumped water

The domain of the function is split into E intervals, indexed with $e = \{1, \ldots, E\}$. A generic interval $e \in \mathcal{E}_{\overline{h}}$ is defined by the partition of the domain $\left[Qp^{max}_{\overline{h},e-1}, Qp^{max}_{\overline{h},e}\right]$ and the image $\left[pp^{max}_{\overline{h},e-1}, pp^{max}_{\overline{h},e}\right]$. Within a generic interval $e \in \mathcal{E}_{\overline{h}}$, the relationship between the power consumption of the pump and the pumped water is imposed to be linear and it is described by the slope coefficient defined in (4):

$$\eta p_{\overline{h},e} = \frac{Qp^{max}_{\overline{h},e} - Qp^{max}_{\overline{h},e-1}}{pp^{max}_{\overline{h},e} - pp^{max}_{\overline{h},e-1}} \qquad \forall e \in \mathcal{E}_{\overline{h}} \tag{4}$$

Consequently, the power required by the pump $pp_{\overline{h},k}$ at the upstream power station $\overline{h}$ at each sub-interval k, is formulated as in (5), while the relative pumped water $qp_{\overline{h},k,e}$ is limited by (6), where $Qp^{max}_{\overline{h},e}$ indicates the maximum water that can be pumped for each segment e:

$$pp_{\overline{h},k} = \sum_{e \in \mathcal{E}_{\overline{h}}} \frac{qp_{\overline{h},k,e}}{\eta p_{\overline{h},e}} \qquad \forall k \in \mathcal{K} \tag{5}$$

$$0 \leq qp_{\overline{h},k,e} \leq Qp_{\overline{h},e}^{max} \qquad \forall k \in \mathcal{K}, \forall e \in \mathcal{E}_{\overline{h}} \tag{6}$$

Moreover, it is important to account for the cavitation effect while in pump mode. Hence, the dependence of the pumping functioning with respect to the water levels inside the reservoirs has been considered. This issue is implemented by means of a state-dependent constraint on the water pumped by the pump $qp_{\overline{h},k,e}$ where the state variables considered are the water volumes inside the downstream reservoir $\underline{h}$ from which the pump $\overline{h}$ is subtracting water. Since the reservoir volumes are known only at the beginning of the stages, the constraint is formulated as in (7). Here, the water volume used as reference threshold is the one at the end of the previous week $v_{\underline{h},k=K}^{t-1}$: if the water volume inside the downstream reservoir $\underline{h}$ happens to go below a certain threshold $\underline{V}_{\underline{h}}$, the pump is not allowed to pump water for all the K steps of the incoming week t.

$$\sum_{e \in \mathcal{E}_{\overline{h}}} qp_{\overline{h},k,e} = 0 \qquad if\ v_{\underline{h},k=K}^{t-1} \leq \underline{V}_{\underline{h}} \qquad \forall k \in \mathcal{K} \tag{7}$$

Depending on the current state of the water volume, the constraint is activated in the mathematical formulation before the optimization problem is solved at each stage t.

3.2 Environmental constraints

The proposed model acknowledges two additional constraints dealing with environmental issues related to the water inside the reservoirs and the surrounding environment. In particular, the first constraint regards the quality-related environmental standard of the flow downstream the hydropower plants; the second constraint deals with the frequent water level fluctuations inside the reservoirs caused by the operation of the hydropower system. These two issues are translated into a set of mathematical constraints (8, 9) that the optimal operation of the hydropower system must respect. In particular:

- The *minimum environmental flow (MEF)* $b_{h,k}$ [m^3/s] in (8) indicates the minimum amount of water that has to be released from the reservoir h at each sub-interval k in order to sustain the downstream ecosystems. The MEF may be active only in specific weeks of the year:

$$b_{h,k} = Q_h^{min} \qquad \forall t \in \mathcal{T}_{MEF} \subset \mathcal{T} \tag{8}$$

- The *ramping constraints* aim at reducing possible fast and high variations of the water levels inside the reservoirs pursuant to the operations of the hydropower system. Since the optimization model proposed in this work considers

the water volumes $v_{h,k}$ as decision variables, the changes in water levels inside the reservoirs are formulated as changes in water volumes as in (9). The variations in water volumes from one sub-interval $k-1$ to the next k are bounded by the downward and upward ramping rates, v_v^- and v_v^+ respectively and both are expressed in Mm^3. In this specific case, the ramping constraints are imposed to be active along the whole planning period.

$$v_v^- \leq v_{h,k} - v_{h,k-1} \leq v_v^+ \qquad \forall t \in \mathcal{T} \tag{9}$$

3.3 Scheduling algorithm

As illustrated in Figs. 2 and 3, the execution of the Scheduling Algorithm is nested in the SDP Algorithm and the FS Algorithm, respectively. The Scheduling Algorithm requires the solution of a multi-stage revenue maximization problem where the hydropower system is assumed to be a price-taker agent operating in a competitive energy market; thus, the operation of the hydropower system does not affect the market clearing.

Figure 5 illustrates the procedure for running the Scheduling Algorithm. For both the SDP and FS algorithms, the corresponding input values are read and the optimization problem (10–20) is built. The algorithm checks if the limitations on the pumping capabilities (Check 1) or if any of the environmental constraints (i.e., SCWA and ramping constraints indicated with Check 2 and Check 3 respectively) are required and solves the optimization problem subject to the applicable set of constraints.

Scheduling Algorithm

- read corresponding inputs
- build the optimization problem (10)-(20)
- run Check 1 Algorithm
- run Check 2 Algorithm
- run Check 3 Algorithm
- solve the complete formulation of the optimization problem
- print outputs

Fig. 5 Pseudocode of the Scheduling Algorithm

The objective function $\alpha_t(s^p, s^u_{h,t,l})$ of the above-mentioned optimization problem is expressed by (10).

$$\alpha_t(s^p, s^u_{h,t,l}) = max\Bigg\{ F^H \lambda_t \sum_{k\in\mathcal{K}} \theta_{t,k} \left[\sum_{h\in\mathcal{H}} p_{h,k} - pp^-_{\overline{h},k} \right] - C^S \sum_{k\in\mathcal{K}} \sum_{h\in\mathcal{H}} f_{h,k} \\ -C^C \sum_{k\in\mathcal{K}} \sum_{h\in\mathcal{H}} \left(res^+_{h,k} + res^-_{h,k} + mef_{h,k} \right) + \alpha_{t+1} \left(v_{h\in\mathcal{H},k=K}, s^u_{h,t+1,l} \right) \Bigg\} \tag{10}$$

$$\alpha_{t+1} = \sum_{n\in\mathcal{N}} \sum_{m\in\mathcal{N}} \gamma_{n,m} FV_{n,m} \tag{10a}$$

Equation (10) maximizes the revenue from operating the hydropower system at the current stage t, considering all the actions taken at each of the sub-intervals k and the expected future profit for stage $t+1$. The expected future profit α_{t+1} is a non-convex function expressing the expected value of maintaining a certain amount of water stored in the reservoirs at the end of the stage t and it depends on both endogenous (s^p) and exogenous ($s^u_{h,t,l}$) state variables of the system. Moreover, the objective function (10) considers the power produced by the turbines $p_{h,k}$ at each sub-interval k and the power used to operate the pump $pp^-_{\overline{h},k}$.

The weekly energy prices λ_t, expressed in €/MWh, are obtained from the Markov model described in Sect. 2.2 and they are distributed along the K sub-intervals by means of a scaling factor $\theta_{t,k}$ to maintain a generic daily pattern. The numerical values are courtesy of the Norwegian University of Science and Technology (NTNU). The values of $\theta_{t,k}$ have been used in this paper only as input parameters to the optimization model. Moreover, since the power is expressed in MW and the electricity price in €/MWh, the conversion factor F^H—which considers the number of hours within each sub-interval k—is used to express the objective function in €. The spillage of water $f_{h,k}$—which is used to discharge the surplus of water when the water volumes inside the reservoir have exceeded their maximum capacity—is penalized with a cost C^s. Moreover,$res^+_{h,k}$ and $res^-_{h,k}$ are two variables included both in the objective function (10) and in the ramping constraints (29) as penalizing factors. This has been done to provide a higher degree of flexibility to the operation of the hydropower system during the wet season. As a matter of fact, in cases of high-water inflows, it might be difficult to maintain the water level fluctuations within a given range and the hydropower system is allowed to violate the restriction on maximum water level variations by paying a penalty fee C^c. Finally, $mef_{h,k}$ is a slack variable included also in Eq. (20) which ensures the requirements on the MEF even during the restriction periods on SCWA.

The non-convex characteristics of the expected future value α_{t+1} is overcome by formulating the function as a linear combination of the weighting variables $\gamma_{n,m}$—bounded to the discrete water volumes of the reservoirs—and the expected future profit points ($FV_{n,m}$) which in turn are dependent on the WVs (10a). The indices n and m refer to the volume segments in the upper and in the in lower reservoir respectively. Hence, a Special Order of Sets (SOS2) is used to approximate α_{t+1} into a piecewise linear function. A more detailed description of the methodology used can be found in [20].

The water volumes inside the reservoirs are subject to the constraints described by (11a–14).

$$v_{\overline{h},k} - v_{\overline{h},k-1} + F^C\left[\left(\sum_{d\in\mathcal{D}_{\overline{h}}} q_{\overline{h},k,d} + f_{\overline{h},k} + b_{\overline{h},k} - \sum_{e\in\mathcal{E}_{\overline{h}}} qp_{\overline{h},k,e} Pd_{\overline{h}}\right)\right] = \varphi_{\overline{h},k} Y_{\overline{h},t} \qquad \forall k \in \mathcal{K} \tag{11a}$$

$$v_{\underline{h},k} - v_{\underline{h},k-1} + F^C\left[\left(\sum_{d\in\mathcal{D}_{\underline{h}}} q_{\underline{h},k,d} + f_{\underline{h},k} + b_{\underline{h},k} - \sum_{e\in\mathcal{E}_{\overline{h}}} qp_{\overline{h},k,e} Pd_{\underline{h}}\right) - \sum_{d\in\mathcal{D}_{\overline{h}}} q_{\overline{h},k,d} + f_{\overline{h},k} + b_{\overline{h},k}\right] = \varphi_{\underline{h},k} Y_{\underline{h},t} \qquad \forall k \in \mathcal{K} \tag{11b}$$

$$V_h^{min} \le v_{h,k} \le V_h^{max} \qquad \forall k \in \mathcal{K}, \forall h \in \mathcal{H} \tag{12}$$

The equality constraints (11a and 11b) express the water mass balance for the upstream reservoir $\overline{h}$ and for the downstream one $\underline{h}$, respectively. When considering (11a), $v_{\overline{h},k}$ indicates the water volume of the upstream reservoir $\overline{h}$ at the end of the sub-interval k while $v_{\overline{h},k-1}$ indicates the water volume at the end of the sub-interval $k-1$. The same considerations can be done for the downstream reservoir $\underline{h}$ in Eq. (11b). In the FS algorithm, when considering the first sub-interval ($k = 1$) of the first week ($t = 1$), the water volumes $v_{h,k-1}$ of both the reservoirs assume the value of $\overline{v}_{h,0}$ which is treated as an input parameter:

$$v_{h,k=0}^{t=1} = \overline{v}_{h,0} \qquad \forall h \in \mathcal{H} \tag{13}$$

Considering the first sub-intervals ($k = 1$) of the following weeks ($t > 1$), $v_{h,k-1}$ assumes the value of the water volumes at the end of the previous stage $t-1$:

$$v_{h,k=0}^{t} = v_{h,k=K}^{t-1} \qquad \forall h \in \mathcal{H} \tag{14}$$

Considering the upstream reservoir $\overline{h}$ in (11a), $Y_{\overline{h},t}$ indicates the total weekly incoming water inflows, $q_{\overline{h},k,d}$ the water discharged from the turbine, $f_{\overline{h},k}$ the spilled water and $b_{\overline{h},k}$ the MEF. Similarly, the water mass balance in (11b) considers the water outflows from the downstream reservoir $\underline{h}$, thus the water discharged through the turbine $q_{\underline{h},k,d}$, the spilled water $f_{\underline{h},k}$ and the MEF $b_{\underline{h},k}$. Furthermore, besides the total weekly incoming inflow $Y_{\underline{h},t}$, the equation considers also all the incoming water that is discharged from the upstream reservoir $\overline{h}$. Finally, since only $\overline{h}$ is a PSHP, Eqs. (11a) and (11b) consider also the water pumped by the pump $qp_{\overline{h},k,e}$ together with the parameter Pd_h, which indicates its flowing direction. When considering the downstream reservoir $\underline{h}$, $Pd_{h=\underline{h}}$ is equal to -1, indicating that the water is subtracted from the downstream reservoir. When considering the upper reservoir $\overline{h}$, $Pd_{h=\overline{h}}$ assumes the value 1, indicating that the upstream reservoir is receiving water from the downstream one. Note that $\varphi_{\overline{h},k}$ and $\varphi_{\underline{h},k}$

are the inflow distribution factors for the intra-weekly sub-intervals k for the upstream and downstream reservoir respectively and F^C is the conversion factor from m^3/s to Mm^3. As expected, the water volumes of the two reservoirs are maintained between a maximum volume V_h^{max} and a minimum one V_h^{min} by (12).

Moreover, the system is subject to the technical constraints (15–19).

$$p_{h,k} = \sum_{d \in \mathcal{D}_h} \eta_{h,d} q_{h,k,d} \qquad \forall k \in \mathcal{K}, \forall h \in \mathcal{H} \tag{15}$$

$$0 \leq q_{h,k,d} \leq Q_{h,d}^{\max} \qquad \forall k \in \mathcal{K}, \forall h \in \mathcal{H}, \forall d \in \mathcal{D}_h \tag{16}$$

$$pp_{\bar{h},k} = \sum_{e \in \mathcal{E}_{\bar{h}}} \frac{qp_{\bar{h},k,e}}{\eta p_{\bar{h},e}} \qquad \forall k \in \mathcal{K} \tag{17}$$

$$0 \leq qp_{\bar{h},k,e} \leq Qp_{\bar{h},e}^{\max} \qquad \forall k \in \mathcal{K}, \forall e \in \mathcal{E}_{\bar{h}} \tag{18}$$

$$\sum_{e \in \mathcal{E}_{\bar{h}}} qp_{\bar{h},k,e} = 0 \qquad if\ v_{\underline{h},k=K}^{t-1} \leq \underline{V}_{\underline{h}} \qquad \forall k \in \mathcal{K} \tag{19}$$

Constraint (15) represents the relationship between the power produced by the turbines $p_{h,k}$ and the corresponding water discharges $q_{h,k,d}$ which in turn are limited by (16). In a similar way, the relationship between the power absorbed by the pump $pp_{\bar{h},k}$ and the corresponding pumped water $qp_{\bar{h},k,e}$ is expressed by (17) where $qp_{\bar{h},k,e}$ is limited by (18) and (19), as explained in Sect. 3.1. Since the pumping unit is present only in the upper reservoir $\bar{h}$, Eq. (19) considers the water volumes inside the downstream reservoir $\underline{h}$ to regulate the pumping activities. The procedure used to regulate the pumping unit is illustrated in Fig. 6.

```
Check 1 Algorithm
if Pumping Capability ON then
  if v^{t-1}_{h,k=K} ≤ V_h then
    add (19)
  end if
end if
```

Fig. 6 Pseudocode of the Check 1 Algorithm relevant to the constraints on pumping functionality (19)

Finally, Eqs. (20–29) implement the environmental constraints required by the local regulation.

$$b_{h,k} + mef_{h,k} = Q_h^{\min} \qquad \forall k \in \mathcal{K}, \forall h \in \mathcal{H}, \forall t \in \mathcal{T}_{MEF} \subset \mathcal{T} \tag{20}$$

$$\sum_{d\in\mathcal{D}_{\underline{h}}} q_{\underline{h},k,d} = 0 \qquad if\ v^{t-1}_{\underline{h},k=K} < V^{lim}_{\underline{h}} \qquad \forall k \in \mathcal{K}, \forall t \in \mathcal{T}_{env} \subset \mathcal{T} \tag{21}$$

$$\sum_{e\in\mathcal{E}_{\overline{h}}} qp_{\overline{h},k,e} = 0 \qquad if\ v^{t-1}_{\underline{h},k=K} < V^{lim}_{\underline{h}} \qquad \forall k \in \mathcal{K}, \forall t \in \mathcal{T}_{env} \subset \mathcal{T} \tag{22}$$

$$\sum_{d\in\mathcal{D}_{\underline{h}}} q_{\underline{h},k,d} \le \sum_{d\in\mathcal{D}_{\underline{h}}} Q^{\max}_{\underline{h},d} \qquad if\ v^{t-1}_{\underline{h},k=K} + Y_{\underline{h},t} \ge V^{\lim}_{\underline{h}} \qquad \forall k \in \mathcal{K}, \forall t \in \mathcal{T}_{env} \subset \mathcal{T} \tag{23}$$

$$\sum_{e\in\mathcal{E}_{\overline{h}}} qp_{\overline{h},k,e} \le \sum_{e\in\mathcal{E}_{\overline{h}}} Qp^{\max}_{\overline{h},e} \qquad if\ v^{t-1}_{\underline{h},k=K} + Y_{\underline{h},t} \ge V^{\lim}_{\underline{h}} \qquad \forall k \in \mathcal{K}, \forall t \in \mathcal{T}_{env} \subset \mathcal{T} \tag{24}$$

$$v_{\underline{h},k=K} \ge V^{\lim}_{\underline{h}} \qquad if\ v^{t-1}_{\underline{h},k=K} + Y_{\underline{h},t} \ge V^{\lim}_{\underline{h}} \qquad \forall t \in \mathcal{T}_{env} \subset \mathcal{T} \tag{25}$$

$$\sum_{d\in\mathcal{D}_{\underline{h}}} q_{\underline{h},k,d} \le \sum_{d\in\mathcal{D}_{\underline{h}}} Q^{\max}_{\underline{h},d} \qquad if\ v^{t-1}_{\underline{h},k=K} \ge V^{\lim}_{\underline{h}} \qquad \forall k \in \mathcal{K}, \forall t \in \mathcal{T}_{env} \subset \mathcal{T} \tag{26}$$

$$\sum_{e\in\mathcal{E}_{\overline{h}}} qp_{\overline{h},k,e} \le \sum_{e\in\mathcal{E}_{\overline{h}}} Qp^{\max}_{\overline{h},e} \qquad if\ v^{t-1}_{\underline{h},k=K} \ge V^{\lim}_{\underline{h}} \qquad \forall k \in \mathcal{K}, \forall t \in \mathcal{T}_{env} \subset \mathcal{T} \tag{27}$$

$$v_{\underline{h},k} \ge V^{\lim}_{\underline{h}} \qquad if\ v^{t-1}_{\underline{h},k=K} \ge V^{\lim}_{\underline{h}} \qquad \forall k \in \mathcal{K}, \forall t \in \mathcal{T}_{env} \subset \mathcal{T} \tag{28}$$

$$res^{-}_{h,k} + v^{-}_{v} \le v_{h,k} - v_{h,k-1} \le v^{+}_{v} + res^{+}_{h,k} \qquad \forall k \in \mathcal{K}, \forall h \in \mathcal{H} \tag{29}$$

Equation (20) implements the MEF $b_{h,k}$ that must be released from the reservoir h to maintain the quality of the ecosystem downstream the relevant plant. It is worth noting that, in (11a), (11b) and (20), the MEF has been modelled by means of a water route that is independent from the one referring to the energy production. This choice would allow to extend the functionalities of the model without major complexities. In fact, it can be adapted to different configurations and adjusted to satisfy site-specific water allocations (i.e., water supply for civil uses, support irrigation, fish water routes and/or other bypass channels).

The SCWA imposed to the reservoir $\underline{h}$ are described by (21–28). The limitations on the maximum discharge through the turbines and on the maximum water pumped by the pump, as well as the constraint on the pumping functionality (19), are state-dependent constraints which depend on the storage volumes in the reservoirs at the beginning of the stages i.e., the endogenous variable s^p. The SCWA are active only for specific weeks of the year ($t \in \mathcal{T}_{env}$) and only depending on the current state of the system i.e., the water volumes $v^{t-1}_{\underline{h},k=K}$ and the weekly incoming inflows $Y_{\underline{h},t}$. Note that the relevant constraints are added to the formulation before the optimization problem is solved, as illustrated in pseudocode of the Check 2 Algorithm in Fig. 7.

Check 2 Algorithm

if $t \in \tau_{env}$ (SCWA are active) **then**
  if $v_{\underline{h},k=K}^{t-1} \geq V_{\underline{h}}^{lim}$ **then**
    add (26)-(28)
  else if $v_{\underline{h},k=K}^{t-1} + Y_{h,t} \geq V_{\underline{h}}^{lim}$ **then**
    add (23)-(25)
  else
    add (21)-(22)
  end if
end if

Fig. 7 Pseudocode of the Check 2 Algorithm relevant to the SCWA (21–28)

If the water volume at the beginning of the restriction period is below a certain threshold $V_{\underline{h}}^{lim}$, no water is allowed to be discharged through the turbine nor pumped by the pump from the reservoir for energy production purposes and constraints (21) and (22) replace (16) and (18) respectively. When and if the water volume reaches the threshold $V_{\underline{h}}^{lim}$ within the restriction period due to a high weekly incoming water inflow $Y_{\underline{h},t}$, the turbine is allowed to discharge water for energy production and the pump is allowed to pump water: constraints (21) and (22) are relaxed and replaced with (23) and (24) while (25) is added to the problem formulation. Note that (25) is active for the first week in which the storage volume reaches the desired threshold, and it imposes the water volume inside the reservoir to stay above $V_{\underline{h}}^{lim}$ by the end of the stage ($k = K$). Constraints (26) and (27) become active from the following week together with constraint (28) which imposes a minimum regulation volume for all the sub-intervals k of the stage: the discharge of water for power production and the withdraw of water by the pump are permitted as long as the water volume inside the reservoir is kept above the limit.

Finally, (29) represents the ramping constraints which impose the maximum water level variations between two adjacent operating time-steps. Also in this case, the ramping constraints are expressed as function of the water volume of the reservoir at the end of the previous stage $v_{h,k=K}^{t-1}$, where the upward and downward ramping rates are expressed in Mm^3 and given by υ_v^+ and υ_v^-. Therefore, the maximum threshold of the water level variations expressed in meters must be converted in variations in water volumes. Furthermore, it is worth noting that, given the positive υ_l^+ and negative υ_l^- water level variations, the corresponding variations in water volume υ_v^+ and υ_v^- change accordingly to the state of the stored water volume. In fact, because of the irregular shape of the reservoirs, the same variations in water levels correspond to higher variations in terms of water volumes if the reservoirs are almost at their maximum capacity. On the contrary, they correspond to smaller volume variations if the reservoirs are almost empty. In order to find the correct water volume variation required, the maximum storage water volume of the reservoir V_h^{max} has been divided into N_r intervals of water volumes indicated as V_r with $r = \{1, \ldots, N_r\}$. For each generalized interval V_r, V_r^- corresponds to the lower bound while V_r^+ to the

upper one. It is worth noting that $V_r^+ = V_{r+1}^-$. For each interval, the negative υ_v^- and positive υ_v^+ water volume variations corresponding to the required water level variations - υ_l^- and υ_l^+ respectively - are evaluated.

The implementation of such constraint is performed by running the Check 3 Algorithm whose pseudocode is in Fig. 8. Before solving the optimization problem for the stage t, the Check 3 Algorithm determines the predefined intervals of water volumes V_r which include $v_{h,k=K}^{t-1}$ and, in turn, chooses the positive υ_v^+ and negative υ_v^- water volume variations - expressed in Mm^3 - to be added to Eq. (29).

Check 3 Algorithm

if Ramping Constraints are active **then**
  for $r = 1 : N_r$
    if $V_r^- \leq v_{h,k=K}^{t-1} < V_r^+$ **then**
      assign corresponding υ_v^- and υ_v^+ to (29)
      add (29)
    end if
  end for
end if

Fig. 8 Pseudocode of the Check 3 Algorithm relevant to the ramping constraints (29)

4 Assessing the solution of the medium-term scheduling model

As explained in Sect. 2.2, the SDP algorithm computes the 1-year worth set of WVs considering weekly decision stages. In turn, the optimal operation resulting from the solution of the FS algorithm maintains the same temporal weekly resolution $t = \{1, \ldots, T\}$ and the same intra-weekly sub-intervals $k = \{1, \ldots, K\}$. It is worth noting that the selection of weekly stages is typical for medium-term scheduling models. These models are in fact adopted to evaluate the optimal management of the water sources inside the reservoirs for planning periods of several months up to 1 year considering the uncertainties of water inflows and energy prices. To grant a more explicit representation of these stochastic variables while at the same time maintaining an affordable computational time, medium-term scheduling models are usually formulated and solved via SDP algorithms.

Note that, under this approach, the states of the system (e.g., water volumes inside the reservoirs s^p, incoming water inflows and average energy prices $s_{h,t,l}^u$) are known on a weekly basis. Such "infrequent" weekly disclosure of the states of the system may prevent the effective actual enforcement of some of the constraints of the FS algorithm. This issue might be more relevant during those weeks where the constraints depending on the state of the system are particularly binding. As a result, the optimal operation of the system might be affected by an over- or under-estimation of the hydropower system technical constraints and external issues (e.g., water inflows). In turns, the economic performance of the hydropower system might be over- or under- assessed.

Considering the FS algorithm, if the states of the systems—thus the water volumes, the total water inflows, and the average energy prices—are known and assessed more frequently, e.g., on a daily base rather than on a weekly base, the actual enforcement of the constraints involving dependencies on the water levels inside the reservoirs or on the incoming inflows could be implemented more effectively.

An illustrative example is offered in Fig. 9, where the data are taken from actual simulation results. The figure illustrates the evolution of the water volume inside the lower reservoir which is subject to the state-dependent constraint on maximum water abstraction. More specifically, the results report the water volumes evaluated at the stage $t = 24$ over all the K sub-intervals, for a randomly selected scenario among the N_s ones. The blue dotted line indicates the optimal water volumes obtained when solving the optimization problem with weekly stages, while the green solid line illustrates the water volumes obtained when solving the same problem by using daily stages. The state-dependent constraint on maximum water abstraction is active since week $t-1$ but it might not be immediately satisfied because of the low water volumes at the beginning of the week and small external inflows. In this case, the water volume inside the lower reservoir at the beginning of the stage t—indicated by the red square—, is below the threshold limit $V_{\underline{h}}^{lim}$ (horizontal dashed red line). Referring to the Check 2 Algorithm explained in Sect. 3.3, the weekly-stages model evaluates if the water volume reaches the predefined threshold by the end of the week (i.e. in $K = 56$) due to the total weekly incoming inflow $Y_{\underline{h},t}$ and applies (23–25). If so, the constraint on the minimum regulation volume (28) becomes active from the following week ($t = 25$). In the daily-stage resolution instead, the model considers the state of the reservoir volume at the beginning of each day and the corresponding daily water inflow $Y_{\underline{h},z}$ within the week t. Considering the same week t and the same boundary conditions (i.e. the very first initial water volumes $v_{\underline{h},k=0}^{t}$, energy prices and water inflows at every sub-interval k), the predefined threshold $V_{\underline{h}}^{lim}$ is already reached at the end of the first day (for $k = 8$) because of a sufficient amount of daily water inflow, as indicated by the black dot in Fig. 9. The constraints (26) and (27) are immediately activated and the constraint on minimum

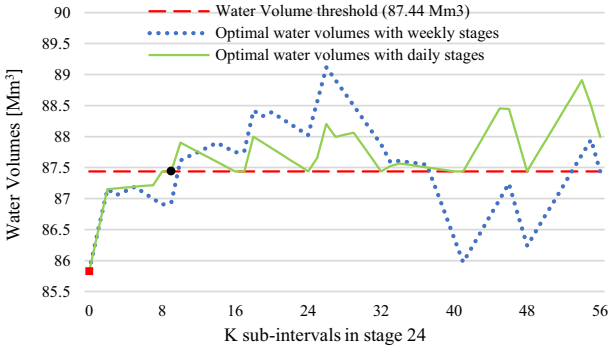

Fig. 9 Evolution of water volume in reservoir subject to state-dependent constraint on maximum water abstraction

volume regulation (28) becomes active for the following days as illustrated by the green solid line.

This first example demonstrates how a finer resolution would permit a more accurate implementation of the state-dependent constraints resulting in a more realistic operation of the hydropower system. However, the sequential resolution of both the SDP and FS algorithm by using daily stages would deviate from the objectives and benefits characterizing medium-term scheduling models. A finer resolution would require changes to the Markov chains for the representation of the daily-based stochastic variables but also changes to the formulation of non-linear relationships characterizing specific constraints and further technical details. Furthermore, the implementation of these changes would largely increase the computational effort. Therefore, to evaluate the accuracy of using a daily-stages approach instead of a weekly one without impacting too much both the computational time and the model structure itself, this paper proposes a new methodology in which the temporal granularity between weekly stages t and $t+1$ is increased only in the FS algorithm. In other words, when moving from one week to the next one, the FS optimizes the operation of the hydropower system taking advantage of a daily update of the relevant WVs, total daily water inflows $Y_{h,z}$, daily average energy prices λ_z, and the very first initial volume states $v^t_{h,k=0}$ evaluated previously in the SDP algorithm. A more detailed setup is graphically explained in Fig. 10; note that $z = \{1, \dots, Z\}$ indexes represent the days within a week, thus $Z = 7$.

The higher granularity introduced by this proposed approach, requires updating the weekly WVs obtained from the SDP algorithm on a daily base, while respecting the boundary values at the beginning and at the end of the reference weeks. Therefore, the following boundary conditions are applied:

$$WV_{z=1} = WV_t; \quad WV_{Z+1} = WV_{t+1} \qquad \text{with Z} = 7 \tag{30}$$

The WVs referring to the remaining days within the week, i.e., $\forall\, z = \{2, \dots, Z\}$, are computed by interpolation [32]:

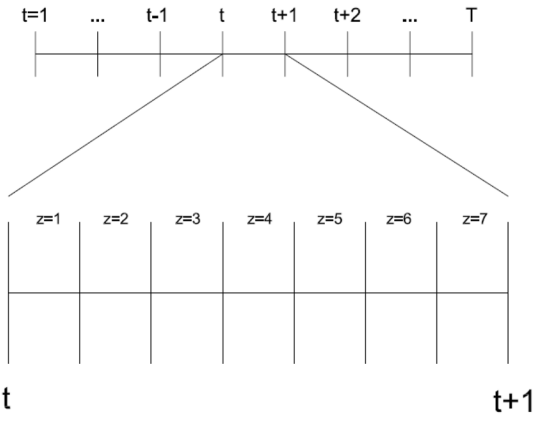

Fig. 10 A graphical illustration of the weekly (top) and daily (bottom) setup

$$WV_z = WV_t + \left[\left(\frac{z-1}{Z}\right)\left(WV_{t+1} - WV_t\right)\right] \tag{31}$$

For the sake of consistency, the objective function (10) is updated below to account for the modifications above:

$$\alpha_z\left(s^p, s^u_{h,z,l}\right) = \max\left\{F^Z \lambda_z \sum_{i\in I}\theta_{z,i}\left[\sum_{h\in\mathcal{H}} p_{h,i} - pp_{\overline{h},i}\right]\right.$$
$$\left. -C^S \sum_{i\in\mathcal{I}}\sum_{h\in\mathcal{H}} f_{h,i} - C^C \sum_{i\in\mathcal{I}}\sum_{h\in\mathcal{H}}\left(res^+_{h,i} + res^-_{h,i} + mef_{h,i}\right) + \alpha_{z+1}\left(v_{h\in\mathcal{H},k=I}, s^u_{h,z+1,l}\right)\right\} \tag{32}$$

The K sub-intervals in the optimization problem based on weekly decisions are distributed equally along the daily stages, providing each stage z with I sub-intervals indexed with $i = \{1, \ldots, I\}$: therefore, the values of natural water inflows from the surroundings and the energy prices, expressed for each of the sub-intervals $k = \{1, \ldots, K\}$, do not change when moving to a daily resolution setup. Furthermore, the water volumes at the beginning of the considered weeks are set to be the same for both the weekly and daily stages resolution, as indicated by the red square in Fig. 9. In other words, considering the week t, the initial water volumes $v^t_{h,k=0}$ of the weekly-optimization problem are equal to the initial water volumes of the first day $z = 1$ of the same week t when considering the daily resolution $v^{z=1}_{h,i=0}$. For the following stages of the daily-optimization problem, thus for $z = \{2, \ldots, Z\}$, the corresponding initial water volumes $v^z_{h,i=0}$ will be equal to the water volumes obtained as result of the optimization problem of the previous day $v^{z-1}_{h,i=I}$. This is to allow a more precise comparison between the weekly and the daily results, maintaining the same initial boundary condition regarding the states of the reservoirs at the beginning of the considered week, as well as the total incoming inflows and average energy prices.

By doing so, the constraints that are dependent on the states of the system do not consider the state values at the beginning of each week t, but the values at the beginning of each day z – thus the water volumes $v^z_{h,i=0}$, the total daily inflows $Y_{h,z}$ and the daily average energy price λ_z-, granting the optimal decisions with higher accuracy.

5 Case studies and results

5.1 Case studies

The optimal scheduling algorithm comprising a PSHP (pertaining to the upper reservoir $\overline{h}$) connected to a HPP (relevant to the lower reservoir $\underline{h}$) subject to technical and environmental constraints proposed in Sect. 3.3 is applied to the actual Rosskrepp-Kvinen hydropower, schematized in Fig. 11. The site is part of the

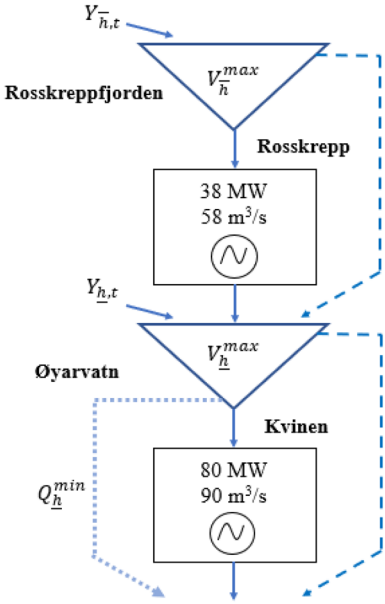

Fig. 11 Schematics of the Rosskrepp-Kvinen hydropower system in its actual configuration

Sira-Kvina watercourse, located in the South of Norway. As per today, the upper hydropower plant comprises the Rosskreppfjorden reservoir with its relative power station—Rosskrepp—while the lower one considers the Øyarvatn reservoir with the Kvinen power station. The upper reservoir has a regulation volume $V_{\overline{h}}^{max}$ of 684.10 Mm^3, while the regulation volume of the lower reservoir is 104.10 Mm^3. Note that, the regulation volume indicates the admissible volume of freshwater used for energy production only. The upper power station is equipped with a Francis turbine whose rated capacity is 38 MW and the maximum water discharge is 58 m^3/s. Another 80 MW Francis turbine is installed in the lower power station, where the maximum water discharge is 90 m^3/s. The discharge water routes for energy production are indicated with blue solid lines, the water routes for spillage with blue dashed lines. The blue dotted line and the parameter $Q_{\underline{h},t}^{min}$ indicate water route for the MEF (20) from the lower reservoir during a certain stage t. The other two arrows, each of them pointing at one reservoir, indicate the weekly water inflows $Y_{h,t}$ at stage t.

It is worth noting that the upstream HPP of the considered site cannot currently operate as a PSHP because the turbine in the upper power station is not able to operate in pumping mode.

Currently, the set of environmental constraints—the state-dependent constraint on maximum discharge through the turbines expressed by equations (21), (23), (25), (26), (28) and the MEF (20)—are applied to the lower reservoir. The threshold values implemented in (21), (23), (25), (26), (28) and (20) together with the reference weeks during which these constraints are enforced, are reported in Table 1.

Table 1 Settings of the environmental constraints in Øyarvatn reservoir.

Environmental constraints	Restriction period (weeks)	Thresholds
State-dependent constraint on maximum discharge (21), (23), (25), (26), (28)	$\forall t \in \{23, \ldots, 38\}$	$V_{\underline{h}}^{\lim} = 87.44\ Mm^3$
Minimum Environmental Flow (20)	$\forall t \in \{25, \ldots, 38\}$	$Q_{\underline{h}}^{\min} = 0.5\ {}^{m^3}/_{s}$
	$\forall t \in \{39, \ldots, 42\}$	$Q_{\underline{h}}^{\min} = 0.2\ {}^{m^3}/_{s}$

The state-dependent constraint on maximum discharge prohibits the water discharge through the turbines for energy production during summer weeks (i.e., 23–38) if the reservoir volume is below the threshold of 87.44 Mm^3. This threshold represents the 84% of the total water capacity of the reservoir. According to the Check 2 Algorithm explained in Sect. 3.3, if the water volume $v_{\underline{h},k=K}^{t-1}$ at the beginning of the restriction period is below the above-mentioned threshold $V_{\underline{h}}^{lim}$ and the total weekly inflows $Y_{\underline{h},t}$ are low, constraint (16) would be replaced by (21): by doing so, the water is impeded to flow through the turbine for energy production purposes. Nonetheless, if the water volume reaches the predefined limit due to large water inflows, constraint (21) is relaxed and replaced by (23). Constraint (25) is also added to ensure the achievement of $V_{\underline{h}}^{lim}$ by the end of that week. From the following weeks, constraint (23) is replaced by (26) while constraint (25) is replaced by Eq. (28) which imposes the regulation on the minimum reservoir volume: the HPP may operate as long as the water volume during all the sub-intervals k is maintained above that given limit. Moreover, the MEF (20) must be released from the lower reservoir to preserve the water flow downstream the plant. A water discharge of 0.5 m^3/s is required from week 25 to week 38, while a MEF of 0.2 m^3/s is imposed from week 39 to week 42. During the remaining weeks of the year, no environmental constraints are set. As per today, there are no ramping constraints (29) applied to the two reservoirs.

Starting from the framework and the numerical settings currently implemented in the Rosskrepp-Kvinen hydropower system, this paper considers four different case studies whose main features are summarized in Table 2. In fact, the proposed paper aims to evaluate how the operation of the current hydropower system might change with the presence of a hydraulic pump unit and/or under the restrictions on water

Table 2 Characteristics of the four case studies.

	Pumping system 38 MW for upper power station (17–19)	SCWA (21–28)	MEF (20)	Ramping constraints (29)
Base Case (BC)		x	x	
Case A	x	x	x	
Case B		x	x	x
Case C	x	x	x	x

level variations. The results of the paper could be considered to evaluate the consequent impact of such water level variations on the surrounding ecosystem. Therefore, the Base Case (BC) considers the current framework and settings of the system where the lower reservoir is subject to the state-dependent constraint on maximum discharge and the MEF, as required by the current regulation [33]. Case A considers the same layout of the BC where, in addition, the electric machine in the upper power station (Rosskrepp) can now function also in pumping mode: the same rated power capacity of 38 MW is assumed for the two operating regimes. The state-dependent constraint on maximum discharge through the turbine has been extended to consider also the water pumped by the pump. Therefore, the optimization problem for Case A considers the SCWA expressed by equations (21–28). Case B and Case C, replicate respectively, the BC and Case A with the additional application of the ramping constraints (29) to the upper reservoir—Rosskreppfjorden. Depending on the site-specific conditions and on the ecological activities present in the reservoirs, local regulations might require the limitation on water level fluctuations in order to reduce the negative impacts on the local surroundings arising from the frequent operation of the hydropower plant. In the case of the Rosskreppfjorden, fast and recurrent water level oscillations—in particular in a PSHP—can negatively affect the spawning activities of fishes and other aquatic species present in the reservoir.

All the numerical simulations concerning the case studies above-mentioned implement a planning horizon of $T = 52$ weeks with an intra-weekly resolution of 3 hours, for a total of 56 sub-intervals K per each weekly stage t. Concerning the SDP algorithm, the endogenous states of the system (s^u), i.e. the upper and the lower water volumes in the reservoirs, have been discretized using $N = 25$ equidistant points, leading to 625 possible couples of volume's combinations evaluated at each stage t. The convergence tolerance ε is set to 10^{-3} €/m^3/s. The discrete Markov chain used for the formulation of the stochastic state variables $s^u_{h,t,l}$ is generated by using inflow data from 30 historical years—from 1981 to 2010—and they are provided by the Norwegian Water Resources and Energy Directorate [33]. The wholesale electricity market prices are instead provided by [34], reflecting a potential 2030 power system in the Nordic scenario. The penalty cost for spillage C^S is equal to 1 M€/m^3/s while the penalty cost for ramping constraints C^C is equal to 0.1 M€/Mm^3. Each of the case studies simulates the same $N_s = 100$ scenarios using the WVs from the corresponding SDP algorithm.

Ramping constraints (29) are imposed only to the upper reservoir—Rosskreppfjorden—with upper and lower bounds for the water level fluctuations set to $\upsilon_l^+ = 0.03$ m and $\upsilon_l^- = -0.03$ m respectively. In this case, as explained in Sect. 3.3

Table 3 Water volume variations in Rosskrepp reservoir

Index for water volume intervals	$r = 1$	$r = 2$	$r = 3$	$r = 4$
Water volume lower bound V_r^- [Mm^3]	0	78	239	452
Water volume upper bound V_r^+ [Mm^3]	78	239	452	684.3
Corresponding water volume variations, v_v^-, v_v^+ [Mm^3]	±0.2364	±0.4815	±0.6380	±0.7734

concerning the Check 3 Algorithm, the maximum capacity of the reservoir has been divided into $N_r = 4$ intervals indexed by r (first row of Table 3). The numerical values of the lower V_r^- and upper V_r^+ bounds of these intervals are in the second and third row of Table 3, respectively. The fourth row expresses the corresponding negative or positive water volume variations v_v^- and v_v^+. For the sake of example, in accordance with the Check 3 Algorithm, for a water volume $V_r^- \leq v_{\overline{h},k=K}^{t-1} < V_r^+$ at the end of the previous stage $t-1$—where $r = 3$ and thus $V_r^- = 239$ Mm^3 and $V_r^+ = 452$ Mm^3 —the positive and negative water volume variations for the stage t are set to be equal to $v_v^+ =+0.6380$ Mm^3 and $v_v^- = -0.6380$ Mm^3 respectively.

The choice of imposing these water level fluctuations has been taken considering the alteration parameters provided in [35].

Finally, the model has been developed using the programming environment Julia 1.7.3 [36] and the JuMP package [37], while the optimization problem has been solved using the CPLEX solver [38]. The case studies were carried out on an Intel(R) Core(TM) i5-52000 processor with 8.0 GB RAM.

5.2 Results

5.2.1 Energy production and revenues

The first set of results assess the annual energy production and the associated revenues under each of the four case studies schematized in Table 2. The authors wish to emphasize that the present study aims to evaluate how both the annual energy production and the total revenues might change when considering the different operating conditions of the hydropower plants, i.e., when considering the presence of a hydraulic pump unit and/or limitations on water volume variations. In other words, this paper only evaluates potential operational benefits without carrying out a full investment analysis which includes the investment costs of the hydraulic pump.

The box and whisker plots in Fig. 12 indicate the variability of the total energy production from the whole system considering all the N_s=100 simulated scenarios.

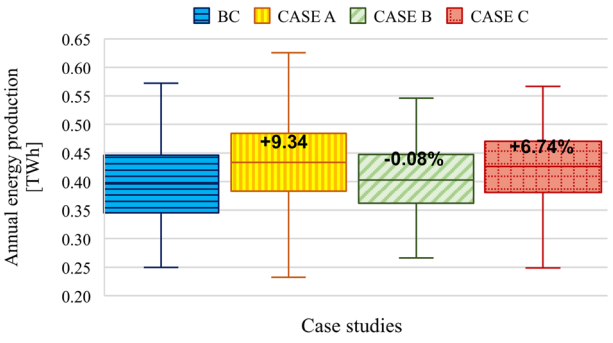

Fig. 12 Annual energy production for Rosskrepp-Kvinen system considering the four case studies

The total energy production is calculated as the sum of the energy output from the turbines of both HPPs along the whole planning period. More specifically, the results consider only the gross energy production which has been injected into the grid, neglecting thus the pumping load. Additionally, the numerical values reported inside the boxes indicate the median of the percentage variation in energy production with respect to the BC (blue box with horizontal pattern) over the set of N_s scenarios. In general, the introduction of a pumping system leads to a higher energy production compared to traditional settings. As expected, the higher boost is granted by Case A (+9.34%)—yellow box with vertical pattern —, due to its increased flexibility stemming from the pumping functionality and the absence of ramping constraints (29). When considering Case B instead (green box with oblique pattern)—which considers a traditional system with the enforcement of the ramping constraints—the results exhibit a decrease of -0.08%. Case C instead (red box with squared pattern), where the ramping constraints are imposed on a PSHP, illustrates an increase in energy production of +6.74%.

Concerning the annual energy consumption, the pumping unit in Case A requires 0.044 TWh to pump 182.68 Mm^3 on average considering all the simulated scenarios. When considering Case C instead, 0.0297 TWh are required to move an average of 122.53 Mm^3 of water among the relevant scenarios. As expected, the energy required by the hydropower system to operate the pump in Case C is lower with respect to Case A due to the presence of the ramping constraints. Clearly, these values are null when considering the Case BC and the Case B.

Similar results occur when considering the whole system's revenues, as illustrated in Fig. 13. The graphs consider the net annual revenues over the N_s scenarios

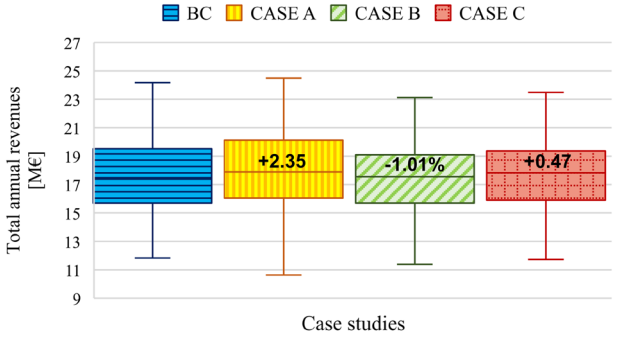

Fig. 13 Total annual revenues from Rosskrepp-Kvinen system

simulated, i.e., the difference between the total revenues resulting from the production of the two turbines and the costs for pumping. The differences in terms of percentage with respect to the BC (blue box with horizontal pattern) are reported inside the boxes and they are calculated in the same way as done for the total energy production. The results evidence that systems operating with a pumping unit exhibit higher incomes with respect to traditional systems, regardless of the implementation

of ramping constraints. Case A (yellow box with vertical pattern) leads to the most remunerative results, with in an increase in the total annual revenues of +2.35%. Case B (green box with oblique pattern) exhibits a decrease in the annual revenues of −1.01% which can be explained by the fact that ramping constraints might redistribute the production from periods of high energy prices to periods of lower energy prices, similar to [28]. It is worth pointing out that Case C (red bow with squared pattern) exhibits an increase in revenues of +0.47 % with respect to the BC, even though the increase is lower than without the ramping constraints (Case A). Therefore, the results confirm that the benefits arising from the use of a pumping system overcome the limitations imposed by the ramping constraints.

5.2.2 Water levels

The evaluation of water level variations and the analysis of their frequencies of occurrence is fundamental for understanding the rate of change in water volumes and the possible setup of ramping constraints. This section illustrates the results regarding the Rosskrepp reservoir considering all the four cases previously described. In particular, Fig. 14 indicates the percentage of sub-intervals k along the whole planning period during which the water level variations can be found in between a certain set of values. Furthermore, in order to have a complete understanding of the results in Fig. 14, it is worth computing, for each range of water level variations, the cumulative amount of water moved. The latter quantity is evaluated as the average—for all the simulated scenarios N_s—of the sum of the water volume variations recorded at the sub-interval k. These metrics are expressed in Mm^3 and are reported in Fig. 14 by means of numbers above each column. It is worth recalling that the same water level variations might result in different variations in terms of water volumes because of the irregular shape of the reservoir.

In general, positive water level variations higher than 0.05 m in 3 hours are relatively frequent in reservoirs where ramping constraints are not present, in particular in those involving a pumping system (they occur for the 5.25% and 11.11% of the time in the BC and in Case A respectively). Similar results can be found for negative water level variations, which occur for 6.42% of the time in the BC (blue column with horizontal pattern) and for 8.79% of the time in Case A (yellow column with vertical pattern). In fact, the results obtained from the FS algorithm have demonstrated that the water levels can increase to values higher than 0.20 m and can decrease down to -0.15 m in 3 hours. However, in few cases, positive and negative water level variations also exceed 0.05 m in Case B (green column with oblique pattern) and Case C (red column with squared pattern) where ramping constraints (29) are imposed. This can be explained by two possible factors. First, the incoming water inflows from the surrounding catchment might be too high with respect to the volume variations permitted, especially during the snow-melting season. To avoid the spillage of potential water for energy production, the hydropower plant prefers to pay a penalty fee and therefore break the ramping constraint. Secondly, these large water level variations could be related to the incorrect selection of the upward v_v^+ and downward v_v^- ramping rates. In fact, similarly to the constraint on the pumping

functionality (19) and to the SCWA (21–28), the ramping constraints (29) consider the water volumes at the end of previous stage $v_{h,k=K}^{t-1}$ as reference values for the optimal choice of v_v^- and v_v^+. However, this could lead to small inaccuracies in the evaluation of the right water volume variations since the water volumes themselves can increase or decrease during the operations within stage t, passing to another interval of volumes, but maintaining the initial water volume variations. A practical solution to overcome this issue, is to increase the number of water volumes intervals N_r (Table 3) to evaluate the optimal water volume variations to be used in Eq. (29) or to directly use the bathymetry of the reservoir.

Furthermore, results highlight that the frequency of occurrence of negative water fluctuations between −0.05 m and 0.00 m, increases pursuant to the introduction of a PSHP in the hydropower system (Case A 42.77% vs. BC 34.56% and Case C 45.87% and Case B 37.2%). An opposite trend is registered considering the frequency of occurrence of positive water level fluctuations between 0.00 m and 0.05 m. Also, the implementation of ramping constraints always increases the positive and negative frequency of occurrence of water level fluctuations (Case B 61.08%. vs. BC 52.86% and Case C 53.01% vs. Case A 36.42%).

In addition, concerning the null water level fluctuations, these occur less than 1% of the time in all the four case studies. The results exhibit that this phenomenon is triggered in two conditions. The first one envisages null water level fluctuations when there are no water inflows from the surrounding catchment and the system is idling (thus the turbine and the pump unit are not working). The second condition refers to a case when the turbine discharges exactly the same amount of the incoming water inflow.

Another important result from Fig. 14 is that, for each of the simulated cases, the sum of all negative cumulative water volume variations is equal to the sum of the overall positive cumulative variations, confirming the correct implementation of the water mass balance during the operation of the plants over the planning horizon. Furthermore, for each of the four case studies, higher or lower frequency of occurrences in the positive and negative intervals do not imply higher or lower fluctuations in absolute terms.

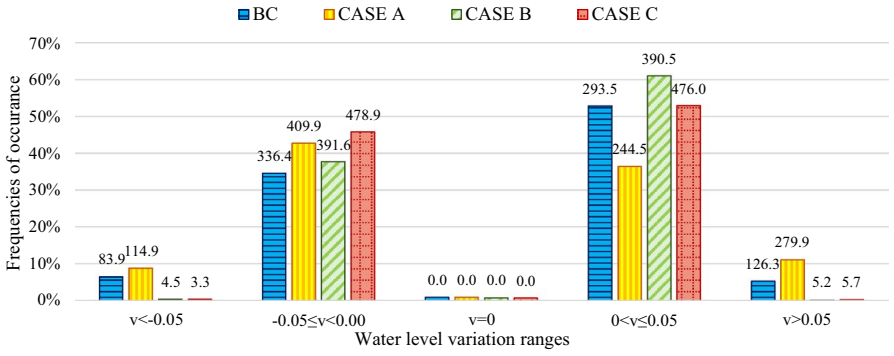

Fig. 14 Water level variations in Rosskrepp reservoir considering a time interval of 3 h

In fact, more frequent water level variations do not necessarily lead to larger cumulative water volume variations. This happens, for instance in Case BC (blue column with horizontal pattern). The negative water level fluctuations between −0.05 m and 0.00 m are less frequent (34.56%) than the positive ones between 0.00 m and 0.05 m (52.86%). Nevertheless, the overall negative cumulative water volume variations are higher than the positive ones, corresponding to 336.4 Mm^3 and 293.5 Mm^3 respectively. Similarly, in Case A positive water level variations higher than 0.05 m occur for the 11.11% of the time and correspond to an overall water cumulative volume variation of 279.9 Mm^3. On the other hand, positive water level variations lower than 0.05 m happen for the 36.42% of the time but they correspond to a lower amount of cumulative water volume variation (244.5 Mm^3).

Moreover, it is worth noting that, when considering the sum of the positive cumulative water volume variations and the sum of the negative ones, these are higher in Case A with respect to the Case BC (524.4 Mm^3 and 419.8 Mm^3 respectively). This is consistent with the presence of a pumping system: the natural inflows and the water pumped by the pump might increase the overall water entering the reservoir, leading to positive volume variations. Consequently, because of the higher availability of water inside the reservoir for energy production, the turbines work more frequently thus increasing the overall negative water volume variations. A similar situation occurs in cases where ramping constraints are imposed: Case C exhibits more consistent cumulative water volume variations (481.7 Mm^3) with respect to Case B (395.7 Mm^3) due to the presence of a pumping unit.

This consideration is further highlighted in Case C (red column with squared pattern). The negative water level variations between −0.05 m and 0.00 m appear for the 45.87% of the time and correspond to a cumulative water volume variation of 478.9 Mm^3. On the contrary, the positive water level variations between 0.00 m and 0.05 m occur more frequently (53.01%) but correspond to a lower value of cumulative water volume variations i.e., 476.0 Mm^3. Even though positive variations are more frequent than the negative ones, the corresponding cumulative water volume variations are lower.

Regardless the possible implementation of ramping constraints, the results of the paper have highlighted fundamental differences already due to the fact that a traditional hydropower system (only with HPPs) is equipped with a PSHP. Results indicated that a hydropower system with a PSHP can effectively boost both the annual energy production and the annual net revenues—accounting for the energy cost sustained during the pump-mode operation—with respect to the traditional system with only HPPs.

Considering the N_s simulated scenarios, which are common to all the case studies, the results indicated that the median energy production can increase up to 9.34% with respect to a traditional system, while the median value of annual revenues can increase up to 2.35%. This is further confirmed by the cumulative water volume variations evaluated during the planning horizon. Due to the presence of a pumping unit, the cumulative water volume variations are more frequent with a PSHP with respect to a traditional HPP (524.4 Mm^3 and 419.8 Mm^3 respectively). Besides the natural inflows entering the reservoir, the additional water inflow due to the pumping unit increments the water availability in the reservoir. Consequently, driven by a

larger potential for energy production, the turbine tends to operate more frequently leading to larger energy production and annual revenues.

Nevertheless, it is worth reminding that the previous results considered only the potential increase in operation revenues from operating the existing system with a pumping unit. It would still be necessary to consider all the relevant investments costs in order to have a full financial analysis on the actual feasibility and profitability of retrofitting an existing conventional HPP with a PSHP. Besides the costs for purchasing the relevant machineries, additional expenses accounting for civil works (i.e., enlargement of power station or construction of additional tunnels), permits, design phases as well as the installation of new monitoring systems should also be considered.

5.2.3 Results from FS algorithm with daily stages

With respect to the methodology proposed in Sect. 4, two specific weeks of the year have been chosen and solved with a daily-stages approach. The system's layout considered is the one of Case C which takes into account a hydropower system equipped with a PSHP where the upper reservoir is subject to the ramping constraints (29). Now the FS algorithm considers a daily optimization problem (10–29) where each stage z is divided into $I = 8$ sub-intervals of 3 hours each. The main characteristics of the weeks are described in Table 4.

The two above-mentioned weeks have been chosen because of the different implementation of the state-dependent constraint on maximum water abstraction (21–28). As explained in Sect. 3.3, the constraint is applied differently according to the states of the system i.e., initial water volumes and total water inflows, at the beginning of the stage. Week 23 indicates the beginning of the snow-melting period, and it is the first week for which the limitation on the water discharged through the turbines and on the water pumped by the pump for energy production is active. Week 34 instead represents a mid-summer week for which the state-dependent constraint on maximum water abstracted from the reservoir has long been present and during which the water volumes inside the reservoirs are kept above the predefined threshold limit. Moreover, a MEF of 0.5 m^3/s is required.

Fig. 15 reports the percent variation in energy production and in revenues when using the FS algorithm with daily stages compared to weekly-stages, evaluated

Table 4 Simulated weeks for a daily-stages approach

Weeks	Characteristics
23	Early summer First activation week of state-dependent constraint on maximum water abstraction from the reservoir No MEF
34	Mid-summer, high water inflow period State-dependent constraint on maximum water abstraction is active MEF = 0.5 m^3/s

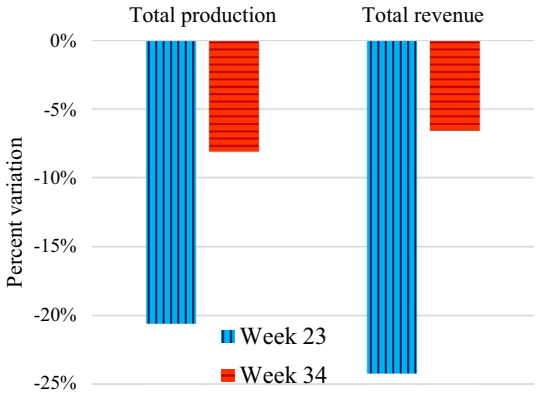

Fig. 15 Differences in percentage in energy production and in revenues between daily and weekly stages

over the N_s scenarios simulated. The results demonstrate that decreasing the time length between stages may not necessarily improve the results despite a more accurate implementation of the constraints and that the differences in the outcomes between two different resolutions might be more accentuated in specific periods of the year.

When considering week 23 (blue column with vertical pattern), in which the state-dependent constraints on maximum water abstraction from the reservoir should be activated for the first time, the results obtained with the daily-stages approach exhibit a decrease of −20.59% in energy production compared to the results obtained with a weekly-stage approach. Similarly, there is a decrease of −24.21% in the total revenues of this week. On the other hand, when considering week 34 (red column with horizontal pattern), during which the state-dependent constraint on maximum water abstraction from the reservoir has long been present and the water volumes at the beginning of the week are already above the given threshold, the differences are smaller. In fact, the daily-stages simulations register a decrease of −8.06% in the energy production and a reduction of −6.55% in the revenues.

This could be explained by the fact that knowing the states of the system daily—thus the water volumes at the beginning of each of the stages $v_{h,i=I}^{z-1}$ and the daily total water inflows $Y_{h,z}$—the state-dependent constraint on maximum water abstraction is applied more accurately with respect to a weekly resolution. Given a more frequent knowledge of the state variables and of the WVs—which have been previously calculated with (31)—the system might find a different optimal operation that maximizes the revenues. Consequently, the amount of water discharged and pumped might change with respect to the weekly resolution and lead to different water volumes inside the reservoirs. This effect is clearly exhibited in Figs. 16 and 17 which illustrate the optimal water volumes evaluated with weekly (blue dotted line) and daily resolution (green solid line) for week 23 and week 34 respectively. The endogenous state variables—thus the initial water volumes inside the reservoir—are represented by the red squares for the weekly resolution and by the black diamonds for the daily one. At the beginning of week 23, the initial water volume (red square) is below the predefined

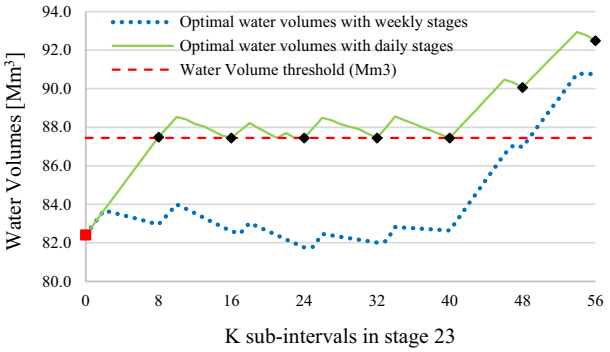

Fig. 16 Evolution of the optimal water volumes in week 23 considering weekly and daily resolution

threshold as shown in Fig. 16. Considering the high daily incoming water inflows, (23–25) are effectively applied with the daily-resolution: the predefined lower threshold (red dashed line) is reached already at the end of the first day (at sub-interval $k = 8$). With a weekly resolution instead, given the high weekly incoming inflow, the system releases water for power production—Eqs. (23) and (24)—and reaches the predefined threshold by the end of the week (thus for $k = 56$) as required by Eq. (25).

Instead, in week 34 the state-dependent constraints on maximum water abstraction through the turbine and the pump (26, 27) and the relative regulation on minimum volume (28) are already strongly consolidated. As a result, the differences in water volumes are less accentuated, as illustrated in Fig. 17, suggesting that the overall optimal operation evaluated with a daily resolution does not significantly differ from the one obtained with weekly stages.

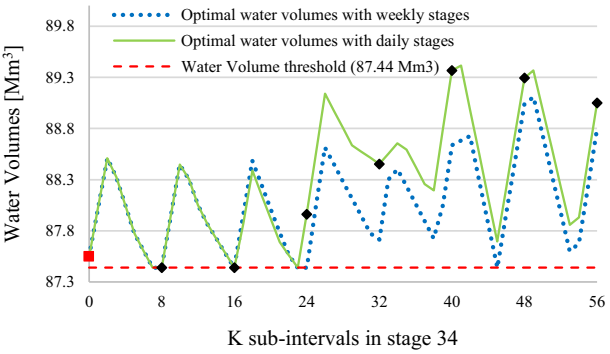

Fig. 17 Evolution of the optimal water volumes in week 34 considering weekly and daily resolution

In conclusion, the results confirm that the weekly model might overestimate the total energy production and revenues from the hydropower system. Especially, the less precise knowledge of the states of the system may cause inaccuracies in the implementation of state-dependent constraints in the FS algorithm when changes in the system's states change the optimization problem.

5.2.4 Assessment on the interpolation procedure

As mentioned in Sect. 1.1, the main drawback of SDP algorithms is the computational burden to solve them, which increases with the number of state variables and with an increase in their discretization.

This paper analyses the main differences, both in the computational time and in the effectiveness of the interpolation procedure used to evaluate the water volumes at the end of the weekly stage. When solving the optimization problem, the storage water volumes calculated at the end of the stage $v_{h,k=K}$ are linked to the discretized endogenous variables s^p through an interpolation procedure. Within this purpose, each of the reservoirs has been discretized by using the same number of points N, indexed with $s = \{1, \ldots, N\}$, for a total of N^2 possible combinations of water volumes states. All the s segments discretizing the same reservoir h have the same water volume and they are indicated with $\sigma^s_{h,N}$ [Mm^3]. To assess the effectiveness of the above-mentioned interpolation procedure, the same case study and same scenarios have been simulated considering 5 different combinations of discretized segments. Table 5 summarizes the values of $\sigma^s_{h,N}$ for both the reservoirs considering the different discretization combinations.

When solving the optimization problem, the optimal water volumes $v_{h,k}$ are found to be inside one of the s segments above-mentioned. Figure 18 provides an illustrative example for the upper reservoir $\overline{h}$. While $\sigma^{s=2}_{\overline{h},N}$ indicates the water volume of the discretized segment $s = 2$ using $N = 5$ discretization points, the corresponding upper and the lower bounds – still expressed in Mm^3 – are indicated with $\overline{\omega}^{s=2}_{\overline{h},N=5}$ and $\omega^{s=2}_{-\overline{h},N=5}$ respectively. More precisely, the water volume $v_{\overline{h},k}$ is more likely to be found in between one of the two halves ($\frac{\sigma^{s=1}_{\overline{h},N=5}}{2}$) composing the corresponding volume segment s. The same considerations are valid for the lower reservoir $\underline{h}$.

Table 5 Volume segments for the two reservoirs, considering five discretization combinations

Combination	Total number of points N^2	Discretized volume segment for upstream reservoir $\sigma^s_{\overline{h},N}$ [Mm^3]	Discretized volume segment for downstream reservoir $\sigma^s_{\underline{h},N}$ [Mm^3]
5×5	25	171.03	26.03
10×10	100	76.01	11.57
15×15	225	48.86	7.44
20×20	400	36.01	5.48
25×25	625	28.50	4.34

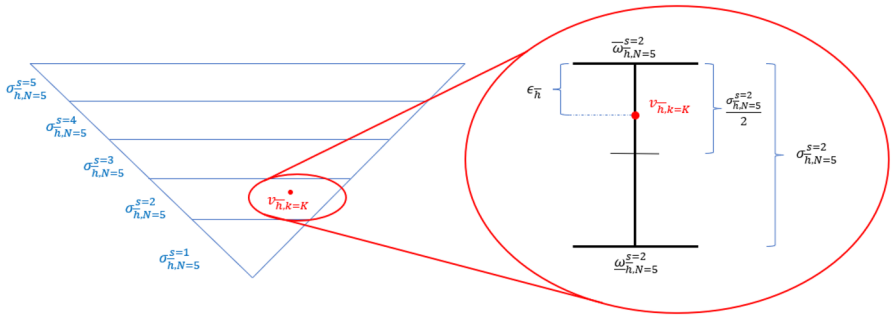

Fig. 18 Graphical representation of $v_{\overline{h},k}$ and of the corresponding discretized volume segment s

In order to give a quantitative measure of the impact of a finer volume discretization on the interpolation procedure for the water volumes, the performance index PI (33) is used:

$$PI = \left[\frac{\epsilon_{\overline{h}} \times \frac{\sigma^{s}_{\overline{h},N=5}}{2} + \epsilon_{\underline{h}} \times \frac{\sigma^{s}_{\underline{h},N=5}}{2}}{\frac{\sigma^{s}_{\overline{h},N=5}}{2} + \frac{\sigma^{s}_{\underline{h},N=5}}{2}} \right] \tag{33}$$

Where ϵ_h indicates the deviation from the water volume $v_{h,k=K}$ of the reservoir h at the end of the stage t from the closest extremes $\overline{\omega}^{s}_{h,N}$ or $\underset{-}{\omega}^{s}_{h,N}$ of the water segment s to which it belongs to, as illustrated in Fig. 18. Moreover, the equation considers the values of $\frac{\sigma^{s}_{\overline{h},N=5}}{2}$ and $\frac{\sigma^{s}_{\underline{h},N=5}}{2}$ which indicate the half of the volume segment s for the upper and lower reservoir respectively when using a discretization of $N = 5$. This allows to have the same reference points as unit of measure and enables a more proper comparison between the different discretization combinations. Clearly, the higher the number of discretization points N is, the finer the water volumes segments $\sigma^{s}_{h,N}$ will be. The same trend regards the effectiveness of the interpolation procedure.

Figure 19 indicates the results obtained from Eq. (33) considering all the T weeks simulated. The box and whisker plots illustrate the variability of the PI characterizing the different combinations. As expected, the variation of the PI and the median values over the T stages considered decrease with a finer discretization of the reservoir volumes.

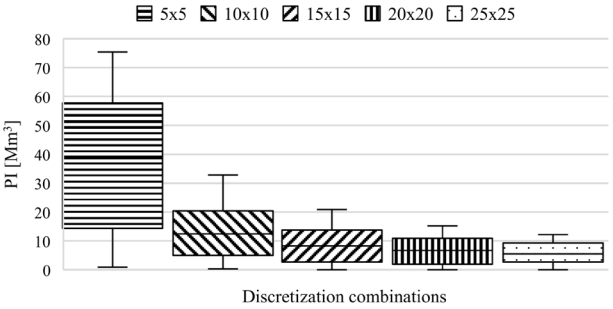

Fig. 19 Performance index for different discretization points

Finally, Fig. 20 indicates the computational time—expressed in hours—required to solve the SDP-FS algorithms for the different combinations of discretization. The graph clearly demonstrates that the computational time increases with a finer discretization of the reservoir volumes. However, it must be noted that these results are obtained with a processor with average computational capabilities (Sect. 5.1). Although the underline trend would be confirmed, the computational time could decrease by using a processor with higher performances.

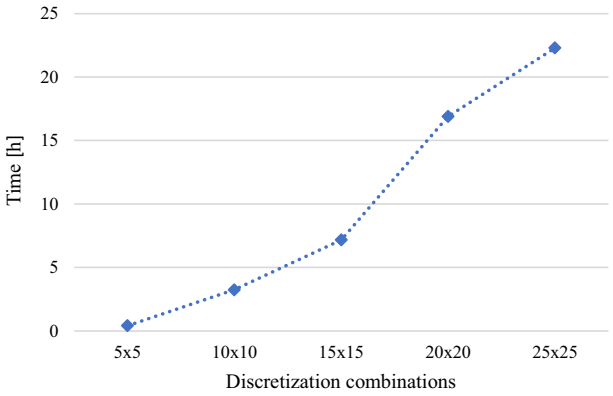

Fig. 20 Computational time for the different discretization combinations

6 Conclusions

This paper presents a SDP-based approach to solve the hydropower scheduling of a hydropower system composed by a PSHP connected to a traditional HPP. More specifically, the model is an extension of a medium-term scheduling model originally developed for a cascade system of two traditional hydropower plants subject to state-dependent constraints on maximum discharge [20]. The implementation of a pumping system with the relative technical constraints and the introduction of two additional environmental constraints—the minimum environmental flow and the ramping constraints—allows the model to consider a pumped-storage hydropower plant connected to a traditional hydropower plant subject to the three environmental constraints all together at the same time. The optimization problem is formulated for a planning horizon of one year with weekly stages and it is solved by using a stochastic dynamic programming algorithm, allowing for the representation of the stochastic variables and the resolution of the non-convex objective function.

The model has been tested on the Rosskrepp-Kvinen hydropower system located in south of Norway. In this context, the paper aims to investigate the potential increment in energy production and annual revenues when operating the system with the addition of a pumping unit and/or in the presence of ramping constraints.

Regardless the implementation of ramping constraints, the results show that the system with a pump unit has a higher total energy production and higher total revenues if compared to the traditional system. For the N_s scenarios simulated, the annual median energy production increases up to +9.34% for a pumped storage system compared to a traditional system, while the increase in the annual median revenue can reach the +2.35%. This increment in energy production is further validated by the cumulative water volume variations evaluated along the planning period. As expected, these are higher with a PSHP with respect to a traditional HPP: the additional water inflows due to the pumping system lead to a higher availability of water inside the reservoir. Consequently, the system operates the turbine more frequently, resulting in higher increments in energy production and therefore in annual revenues. In fact, the hydropower systems with a PSHP may increase the revenues by effectively operating the plant in turbine mode when the wholesale prices reach high values. As explained, the results pertain the operational revenues of the hydropower system and may serve as input, in future work, to run a full investment analysis on the financial viability of upgrading a traditional HPP into a PSHP. This assessment will also have to consider the costs for civil works and for the purchase of the relative machineries.

Moreover, the results demonstrate how ramping constraints can effectively influence the operational scheduling of the system and its economics. For the traditional hydropower plant both the energy production and in the annual revenues decrease (with −0.08% and −1.01% respectively) when the ramping constraints are imposed, suggesting the redistribution of energy production along periods of low energy prices. Still, even though the ramping constraints were found to reduce the energy production and the total revenue, there was an increase in the energy production

of +6.74% and an increase in the annual revenues of +0.47% for pumped-storage systems with ramping constraints compared to the traditional system without the constraint.

For what concerns the water levels inside the reservoirs, systems operating without the restriction of ramping constraints tend to have higher variations, with increments and decrements higher than 0.15 m in the 3-hour interval. In systems where ramping constraints are imposed instead, the water level variations tend to stay in between the required range for most of the time. However, there are some cases in which this limitation cannot be fully satisfied because of high water inflows or because of an inaccurate choice of the right water volume variations in the optimization problem.

Secondly, the results obtained from the case study with resolution on the stages in the forward simulation, demonstrated how the use of a medium-term model might underestimate the effect of constraints and overestimate some technical considerations and thereby the economic performance of the power system. For this particular case study, the results show that a more accurate knowledge of the state variables and therefore a more accurate implementation of the state-dependent constraints, leads to a global decrease both in the energy production and in the total revenues. Furthermore, the analysis regarding the discretization level of the water volumes clearly demonstrated how the effectiveness of the interpolation procedure used for the evaluation for the water volumes increases with an increasing number of discretization points, but at a higher computational cost.

The results presented in this paper suggest further pathways for further development. First, the additional revenues stemming from the introduction of a pumping unit should contribute to a full investment analysis considering the related investment cost. In addition, the benefits of a pumping functionality should be assessed in a competitive market framework where the PSHP is treated as a price-maker agent. Concerning the modelling exemptions of the PSHP, future studies will refine this analysis by incorporating more detailed description of the relevant technologies of the main electrical machines and components (e.g., converters) and their impact on the outcomes of the analysis. This would allow to acknowledge the flexibility of fully-fed or doubly-fed electrical machines with respect to more traditional fixed-speed pumps. Finally, the optimal operation of the PSHP should consider additional revenue streams such as availability fees for frequency response or other ancillary services. This of course would require an extension of the modelling formulation to account for technical related constraints.

Acknowledgements The authors would like to express their gratitude to the anonymous reviewers for the insightful comments on the manuscript. The research leading to these results is part of the HydroConnect project funded by The Research Council of Norway, Agder Energi, BKK, EnergiNorge, HydroEnergi, Lyse Produksjon, Sira-Kvina Kraftselskap. The Ph.D. work of Asja Alic contributing to this research is supported by the Italian National PhD in Photovoltaics – workpackage: solar intermittency and storage.

Declarations

Conflict of interest The authors declare that they have no known competing financial interests or personal relationships that could have appeared to influence the work reported in this paper.

References

1. IEA - International Energy Agency: IEA. Global Energy Review 202: Assessing the Effects of Economic Recoveries on Global Energy Demand and CO2 Emissions in 2021. April 2021. [Online]. Available: https://www.iea.org/reports/global-energy-review-2021. Accessed Oct 2022
2. Gong, X., Yang, M., Du, P.: Renewable energy accommodation potential evaluation of distribution network: a hybrid decision-making framework under interval type-2 fuzzy environment. J. Clean. Prod. **286**(124918), 4270 (2021)
3. Trovato, V.: System scheduling with optimal time-varying delivery intervals for frequency response. IEEE Trans. Power Syst. **37**(6), 4270–4285 (2022)
4. Telukunta, V., Pradhan, J., Agrawal, A., Sing, M., Srivani, S.G.: Protection challenges under bulk penetration of energy resources in power systems: a review. CSEE J. Power Energy Syst. **3**(4), 365–379 (2017)
5. Trovato, V., Martinez Sanz, I., Chaudhuri, B., Strbac, G.: Preventing cascading tripping of distributed generators during non-islanding conditions using thermostatic loads. Int. J. Electr. Power Energy Syst. **106**(19), 183–191 (2019)
6. Pitorac, L., Vereide, K., Lia, L.: Technical review of existing norwegian pumped storage plants. Energies **13**(18), 4918 (2020)
7. Ma, X., Wu, D., Wang, D., Huang, B., Desomber, K., Fu, T., Weimar, M.: Optimizing pumped storage hydropower for multiple grid services. J. Energy Storage **51**, 104440 (2022)
8. EIA, US Energy Information Administration: Utility-scale batteries and pumped storage return about 80% of the electricity they store. 12 February 2021. [Online]. Available: https://www.eia.gov/todayinenergy/detail.php?id=46756#:~:text=Round%2Dtrip%20efficiency%20is%20the,lost%20in%20the%20storage%20process. Accessed Nov 2022
9. Mattmann, M., Logar, I., Brouwer, R.: Hydropower externalities: a meta-analysis. Energy Econom. **57**, 66–77 (2016)
10. Patocka, F.: Environmental impacts of pumped storage hydro power plants. NTNU—Norwegian University of Science and Technology, Trondheim—Norway (2014)
11. Solvang, E., Charmasson, J., Sauterleute, J., Harb, A., Killingtveit, A., Egeland, H., Andersen, O., Ruud, Ø., Aas, Ø.: Norwegian hydropower for large-scale electricity balancing needs. SINTEF Report—SINTEF Energy Research, 14 Feb 2014
12. Bermúdes, M., Cea, L., Agudo, J.P., Rodrígues, N., Baztán, J.: Numerical modelling of the impact of a pumped-storage hydroelectric power plant on the reservoir's thermal stratification structure: a case study in NW Spain. Environ. Model. Assess. **23**(1), 71–85 (2018)
13. Kobler, U.G., Martin, S.: Ensemble modelling of ice cover for a reeservoir affected by pumped-storage operation and climate change. Hydrol. Process. **33**(20), 2676–2690 (2019)
14. Schäffer, L.E., Adeva-Bustos, A., Bakken, T.H., Helseth, A., Korpås, M.: Modelling of environmental constraints for hydropower optimization problems—a review. In: 17th International Conference on the European Energy Market (EEM), Stockholm, Sweden (2020). https://doi.org/10.1109/EEM49802.2020.9221918
15. Alfredsen, K., Harby, A., Linnansaari, T., Ugedal, O.: Development of an inflow-controlled environmental flow regime for a Norwegian river. River Res. Appl. **28**(6), 731–739 (2012)
16. Helseth, A.: Environmental constraints in seasonal hydropower—survey and feasibility. hydroCen, Trondheim (2019)
17. Helseth, A., Cordeiro Geber de Melo, A.: Scheduling toolchains in hydro-dominated systems. SINTEF Energy Research, Trondheim, Norway (2020)
18. do Prado, J.C., Qiao, W.: A stochastic distribution system market clearing and settlement model with distributed renewable energy utilization constraints. IEEE Syst. J. **16**(2), 2336–2346 (2022)
19. Shang, L., Li, X., Shi, H., Kong, F., Wang, Y., Shang, Y.: Long-, medium-, and short-term nested optimized-scheduling model for cascade hydropower plants: development and practical application. Water MDPI **14**(10), 1586 (2022)
20. Schäffer, L.E., Halseth, A., Korpås, M.: A stochastic dynamic programming model for hydropower scheduling with state-dependent maximum discharge constraints. Renew. Energy Elsevier **194**, 571–581 (2022)
21. Hjelmeland, M.N., Zou, J., Helseth, A., Ahmed, S.: Nonconvex medium-term hydropower scheduling by stochastic dual dynamic integer programming. IEEE Trans. Sustain. Energy **10**(1), 481–490 (2018)
22. Bellman, R.: Dynamic programming and stochastic control processes. Inf. Control **1**(3), 228–239 (1958)

23. Helseth, A., Fodstad, M., Askeland, M., Mo, B., Nilsen, O.B., Pérez-Díaz, J.I., Chazarra, M., Guisández, I.: Assessing hydropower operational profitability considering energy and reserve markets. IET Renew. Power Gener. **11**(13), 1640–1647 (2017)
24. Pérez-Díaz, J.I., Guisández, I., Chazarra, M., Helseth, A.: Medium-term scheduling of a hydropower plant partecipating as a pricemaker in the automatic frequency restoration reserve market. Electr. Power Syst. Res. **185**, 106399 (2020)
25. Côté, P., Arsenault, R.: Efficient implementation of sampling stochastic dynamic programming algorithm for multireservoir management in the hydropower sector. J. Water Resour. Plan. Manag. **145**(4), 05019005 (2019)
26. Guisández, I., Pérez-Díaz, J.I., Wilhelmi, J.R.: Assessment of the economic impact of environmental constraints on annual hydropower plant operation. Energy Policy Elsevier **61**, 1332–1343 (2013)
27. Guisández, I., Pérez-Díaz, J.I., Wilhelm, J.R.: The influence of environmental constraints on the water value. Energies **9**(6), 446 (2016)
28. Niu, S., Insley, M.: On the economics of ramping rate restrictions at hydro power plants: balancing profitability and environmental constraints. ELSEVIER Energy Econom. **39**, 39–52 (2013)
29. Helseth, A., Mo, B., Hagenvik, H.O., Schäffer, L.E.: Hydropower scheduling with state-dependent discharge constraints: an SDDP approach. J. Water Resour. Plan. Manag. **148**(11), 04022061 (2022)
30. Hjelmelnd, M.N., Helseth, A., Korpas, M.: Impact of modelling details on the generation function for a norwegian hydropower producer. J. Phys. **1042**, 012010 (2019)
31. Ikotun, A.M., Ezugwu, A.E., Abualigah, L., Abuhaija, B., Heming, J.: K-means clustering algorithms: a comprehensive review, variants analysis, and advances in the area of big data. Inf. Sci. **622**, 178–210 (2023)
32. Haugen, M., Helseth, A.: Primod—A fundamental short-term model for power system analyses and multi-market price forecasting. SINTEF, Trondheim (2018)
33. NVE - The Norwegian Water Resources and Energy Directorate: Historical water flow data for production planning. 18 06 2021. [Online]. Available: https://nve.no/vann-og-vassdrag/hydrologiske-data/historiske-data/historiske-vannforingsdata-til-produksjonsplanlegging/
34. The Project Bank: New environmental restrictions—overall impact on the power system," The Research Council, [Online]. Available: https://prosjektbanken.forskningsradet.no/en/project/FORISS/309622?Kilde=FORISS&distribution=Ar&chart=bar&calcType=funding&Sprak=no&sortBy=date&sortOrder=desc&resultCount=30&offset=0&Prosjektleder=Solgun%20Furnes
35. Bakken, T., Beck, V., Schönfelder, L., Charmasson, J., Thrane, J., Lindholm, M., Brabrand, A.: Testing and evaluation of HYMO classification system for lakes and reservoirs—proposed new and modified hydromorphological (HYMO) classification system. SINTEF, Trondheim, Norway, (2019)
36. "The Julia Programming Language," 2022. [Online]. Available: https://julialang.org/. Accessed Feb 2022
37. JuMP, "Introduction to JuMP," [Online]. Available: https://jump.dev/JuMP.jl/stable/
38. "IBM CPLEX optimizer," 2022. [Online]. Available: https://www.ibm.com/it-it/analytics/cplex-optimizer. Accessed Feb 2022

Authors and Affiliations

Asja Alic[1] · Linn Emelie Schäffer[2,4] · Marco Toffolon[1] · Vincenzo Trovato[1,3]

✉ Asja Alic
asja.alic@unitn.it

Linn Emelie Schäffer
linnemelie.schaffer@sintef.no

Marco Toffolon
marco.toffolon@unitn.it

Vincenzo Trovato
vincenzo.trovato@unitn.it

[1] Department of Civil, Environmental and Mechanical Engineering, University of Trento, Trento, Italy

[2] Department of Electric Power Engineering, Norwegian University of Science and Technology, Trondheim, Norway

[3] Department of Electrical and Electronic Engineering, Imperial College London, South Kensington Campus, London, United Kingdom

[4] Department of Energy Systems, SINTEF Energy Research, Trondheim, Norway